ORIGINAL RESEARCH
published: 12 April 2019
doi: 10.3389/feart.2019.00060

Geochemistry of CO_2-Rich Gases Venting From Submarine Volcanism: The Case of Kolumbo (Hellenic Volcanic Arc, Greece)

Andrea Luca Rizzo[1]*, Antonio Caracausi[1], Valérie Chavagnac[2], Paraskevi Nomikou[3], Paraskevi N. Polymenakou[4], Manolis Mandalakis[4], Georgios Kotoulas[4], Antonios Magoulas[4], Alain Castillo[2], Danai Lampridou[3], Nicolas Marusczak[2] and Jeroen E. Sonke[2]

[1] Istituto Nazionale di Geofisica e Vulcanologia, Sezione di Palermo, Palermo, Italy, [2] Centre National de la Recherche Scientifique, Géosciences Environnement Toulouse, Toulouse, France, [3] Department of Geology and Geoenvironment, National and Kapodistrian University of Athens, Athens, Greece, [4] Hellenic Centre for Marine Research, Institute of Marine Biology, Biotechnology and Aquaculture, Heraklion, Greece

Edited by:
Guido Giordano,
Università degli Studi Roma Tre, Italy

Reviewed by:
Yuri Taran,
National Autonomous University of Mexico, Mexico
Valerio Acocella,
Università degli Studi Roma Tre, Italy

***Correspondence:**
Andrea Luca Rizzo
andrea.rizzo@ingv.it

Specialty section:
This article was submitted to Volcanology, a section of the journal Frontiers in Earth Science

Received: *01 August 2018*
Accepted: *12 March 2019*
Published: *12 April 2019*

Citation:
Rizzo AL, Caracausi A, Chavagnac V, Nomikou P, Polymenakou PN, Mandalakis M, Kotoulas G, Magoulas A, Castillo A, Lampridou D, Marusczak N and Sonke JE (2019) Geochemistry of CO_2-Rich Gases Venting From Submarine Volcanism: The Case of Kolumbo (Hellenic Volcanic Arc, Greece). Front. Earth Sci. 7:60. doi: 10.3389/feart.2019.00060

Studies of submarine hydrothermal systems in Mediterranean Sea are limited to the southern Italian volcanism, while are totally missing in the Aegean. Here, we report on the geochemistry of high-temperature fluids (up to 220°C) venting at 500 m b.s.l. from the floor of Kolumbo submarine volcano (Hellenic Volcanic Arc, Greece), which is located 7 km northeast of Santorini Island. Despite the recent unrest at Santorini, Kolumbo submarine volcano is considered more active due to a higher seismicity. Rizzo et al. (2016) investigated the He-isotope composition of gases collected from seven chimneys and showed that are dominated by CO_2 (>97%), with only a small air contamination. Here we provide more-complete chemical data and isotopic compositions of CO_2 and CH_4, and Hg(0) concentration. We show that the gases emitted from different vents are fractionated by the partial dissolution of CO_2 in water. Fractionation is also evident in the C-isotope composition ($\delta^{13}C_{CO_2}$), which varies between −0.04 and 1.15‰. We modeled this process to reconstruct the chemistry and $\delta^{13}C_{CO_2}$ of intact magmatic gases before fractionation. We argue that the CO_2 prior to CO_2 dissolution in water had $\delta^{13}C \sim -0.4‰$ and $CO_2/^3He \sim 1 \times 10^{10}$. This model reveals that the gases emitted from Kolumbo originate from a homogeneous mantle contaminated with CO_2, probably due to decarbonation of subducting limestone, which is similar to other Mediterranean arc volcanoes (e.g., Stromboli, Italy). The isotopic signature of CH_4 ($\delta^{13}C \sim -18‰$ and $\delta D \sim -117‰$) is within a range of values typically observed for hydrothermal gases (e.g., Panarea and Campi Flegrei, Italy), which is suggestive of mixing between thermogenic and abiotic CH_4. We report that the concentrations of Hg(0) in Kolumbo fluids are particularly high (~61 to 1300 ng m^{-3}) when compared to land-based fumaroles located on Santorini and worldwide aerial volcanic emissions. This finding may represent further evidence for the high level of magmatic activity at Kolumbo. Based on the geo-indicators of temperature and pressure, we calculate that the magmatic gases equilibrate within the Kolumbo hydrothermal system at about 270°C and at a depth of ∼1 km b.s.l.

Keywords: Hellenic Volcanic Arc, Kolumbo submarine volcano, submarine gases, gas–water interaction, hydrothermal system, CO_2, CH_4

INTRODUCTION

About 80% of Earth volcanism occurs on the ocean floor (Crisp, 1984), which has greatly hindered the understanding of the natural outgassing of volatiles from the Earth's interior and its impact on the environment. Several submarine volcanoes have been discovered in recent decades, and geochemical studies have investigated the current status of submarine magmatic-hydrothermal systems. These studies have focused either on midocean ridges (e.g., Butterfield et al., 1990; Lilley et al., 1993; Von Damm, 1995; Von Damm et al., 1995; Lupton et al., 1999) or subduction-related settings (Taran et al., 1992; Tsunogai et al., 1994; Caracausi et al., 2005; Chiodini et al., 2006; Lupton et al., 2006, 2008; Lan et al., 2010; Rizzo et al., 2016; Stucker et al., 2017; and references therein). To the best of our knowledge, Panarea (Aeolian Islands, Italy) is the only volcanic system in the Mediterranean basin characterized by active submarine emissions for which geochemical studies have provided detailed and comprehensive reconstructions of the gas–water interaction process, the origin of gases and the magmatic-hydrothermal system (Caliro et al., 2004; Caracausi et al., 2005 and references therein; Chiodini et al., 2006; Capaccioni et al., 2007; Tassi et al., 2009, 2014; and references therein). The submarine emissions at Panarea are mainly located at relatively shallow water depths (down to 30 m), thereby providing easy access for gas sampling.

In 2006, an extensive hydrothermal vent field was discovered at a depth of 500 m on the floor of Kolumbo submarine crater (Sigurdsson et al., 2006), 7 km off the northeast coast of the Santorini Island (**Figure 1**) in the southern Aegean Sea, Greece (Nomikou et al., 2012). Kolumbo volcano lies along the Christianna-Santorini-Kolumbo volcanic line (CSK; **Figure 1**) that is in the central part of the Hellenic Volcanic Arc (HVA; Nomikou et al., 2016, 2018). The CSK consists of 23 submarine cones and craters (Nomikou et al., 2012; Hooft et al., 2017), of which Kolumbo is the largest and most-active, and last erupted in 1650 (Cantner et al., 2014). The crater is 1.7 km in diameter and up to 500 m deep, with the shallowest point nowadays being at 18 m b.s.l. (below sea level) (Nomikou et al., 2012). All of these volcanoes belong to the modern HVA formed by the subduction of the African plate beneath the European plate (McKenzie, 1972; Le Pichon and Angelier, 1979). HVA began to form 3–4 My ago (Pe-Piper and Piper, 2007), and it stretches from the Gulf of Saronikos in the northwest to the Kos-Nisyros-Yali Islands complex in the east (**Figure 1**).

The Kolumbo hydrothermal vent field emits CO_2-dominated fluids at temperatures as high as 220°C (Sigurdsson et al., 2006; Carey et al., 2013) and with a clear mantle origin (Rizzo et al., 2016). However, the origin of CO_2 and CH_4, the extent of variability in the geochemistry of gases emitted from different chimneys, and the pressure and temperature conditions of the magmatic-hydrothermal system remain unclear.

This study aims to fill this gap in the knowledge by combining the chemical and isotopic data previously reported for noble gases by Rizzo et al. (2016) with new chemical data from the analysis of Hg(0) and the isotopic compositions of CO_2 and CH_4. We identified and modeled the main processes underlying the alterations in the isotopic composition of magmatic-hydrothermal fluids along the path of their ascent, in order to reconstruct the original chemistry of these gases at the earliest stages of their formation. Finally, we used geo-indicators to elucidate the pressure and temperature conditions of the hydrothermal system feeding the gas vents beneath Kolumbo volcano, and propose a conceptual scheme for the fluid circulation.

PRESENT KNOWLEDGE ABOUT KOLUMBO SUBMARINE VOLCANO

The Kolumbo submarine volcano developed next to Santorini Island (**Figure 1**), and several multidisciplinary studies have been carried out over the last decade to shed light on its plumbing system and activity state. The findings of volcanological and geochemical investigations suggest that there are two distinct plumbing systems beneath the Santorini and Kolumbo volcanic systems (Francalanci et al., 2005; Dimitriadis et al., 2009; Kilias et al., 2013). The depth of the magma chamber beneath Kolumbo has been constrained by seismological and petrological observations to lie at depths of 5–7 km (Dimitriadis et al., 2009, 2010; Konstantinou and Yeh, 2012; Cantner et al., 2014). A more recent petrological study revealed striking geochemical differences (e.g., in Nb/Yb, Zr/Nb, $^{206}Pb/^{204}Pb$, $^{87}Sr/^{86}Sr$, and $^{3}He/^{4}He$) between Kolumbo and Santorini magmas despite their close temporal and spatial associations, supporting the hypothesis that the two magmatic systems have distinct mantle sources (Klaver et al., 2016).

Modern-day microseismicity along the CSK is concentrated beneath Kolumbo at depths of 6–9 km (Bohnhoff et al., 2006; Dimitriadis et al., 2009), with the exception of the unrest at Santorini during 2011–2012 when the seismicity focus migrated within its caldera (e.g., Parks et al., 2012). This confirms that Kolumbo is the most-active volcanic system in the region at the present time (Francalanci et al., 2005; Dimitriadis et al., 2009, 2010; Nomikou et al., 2012; Hubscher et al., 2015). Similar indications come from the presence of intense degassing of hydrothermal vents on the floor of Kolumbo submarine crater

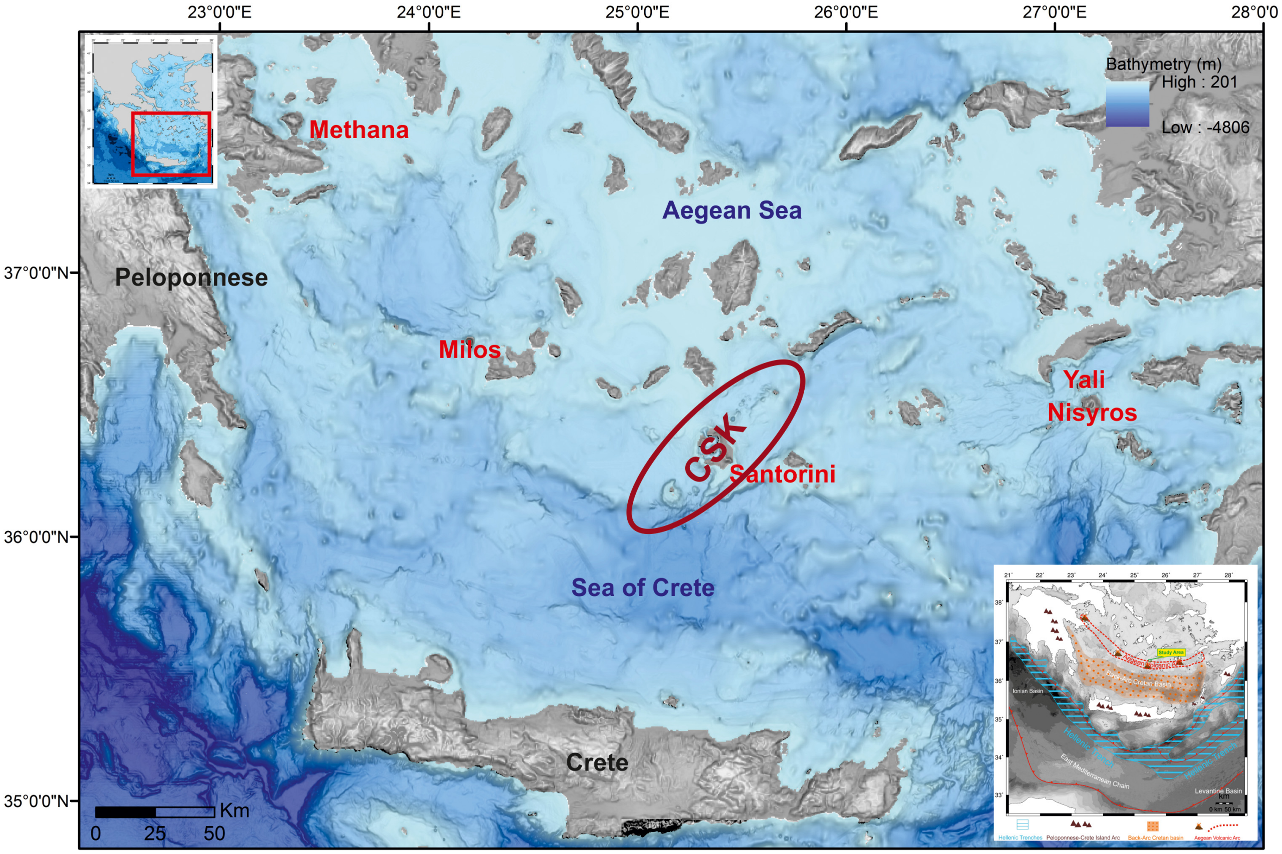

FIGURE 1 | Offshore and onshore topographic map of the Aegean Sea and the location of the main eruptive centers belonging to the modern HVA (Hellenic Volcanic Arc) (modified after Nomikou et al., 2013). Bathymetry is from the EMODNET database (www.emodnet.eu). CSK indicates the Christianna-Santorini-Kolumbo volcanic line. The inset map shows the main geodynamics of the Aegean Sea (Nomikou et al., 2018).

and the geochemistry of these fluids (Sigurdsson et al., 2006; Carey et al., 2013; Rizzo et al., 2016). This intense degassing contrasts with the low-temperature fumaroles observed in the Santorini caldera (Sigurdsson et al., 2006; Rizzo et al., 2015; and references therein).

Sigurdsson et al. (2006) were the first to describe the presence of a widespread hydrothermal vent field on the floor of Kolumbo submarine crater, but only two subsequent geochemical studies have investigated the chemistry of these fluids (Carey et al., 2013; Rizzo et al., 2016). Sigurdsson et al. (2006) and Carey et al. (2013) reported that fluids emitted from the Kolumbo floor are at temperatures up to 220°C and pH ~5 next to the vents, respectively. Carey et al. (2013) also reported the first data for the chemical composition of gas samples collected from two vents, which indicated that these gases are virtually pure CO_2. However, that study focused on the acidification-related hazards that may arise from the dissolution of CO_2 in seawater, which was found to occur within the first 10 m of the water column inside the bowl-shaped crater. This dissolution causes local increases in water density and favors the accumulation of CO_2-rich, acidic waters at the seafloor that do not permit the growth of macrofauna (Camilli et al., 2015), while additional hazards could arise from the abrupt release of gases at the surface.

Rizzo et al. (2016) reported on $^3He/^4He$ measurements of gas samples collected during May 2014 from seven chimneys. Briefly, they constrained the $^3He/^4He$ signature of Kolumbo gases and of the local mantle at 7.0 Ra (where Ra is the atmospheric $^3He/^4He$ equal to 1.39×10^{-6}), which is indicative of a MORB-like mantle. It was subsequently revealed that these values are significantly lower than the $^3He/^4He$ values measured in Santorini fluids and rocks (~4 Ra; Rizzo et al., 2015 and references therein), whereas the observed decrease in the He-isotope signature was attributable to a crustal contamination below the Island. Finally, that study highlighted that $^3He/^4He$ values measured at Kolumbo were the highest ever measured across the entire HAV and indicative of the direct degassing through lithospheric faults.

SAMPLING AND ANALYTICAL TECHNIQUES

During the 4-SeaBioTech survey on RV AEGAEO (Hellenic Centre for Marine Research) during May 2014, seven chimneys bubbling gas phases with variable sustained fluxes were sampled on the floor of Kolumbo submarine crater with the Greek Max Rover remotely operated vehicle (ROV) (**Figure 2**).

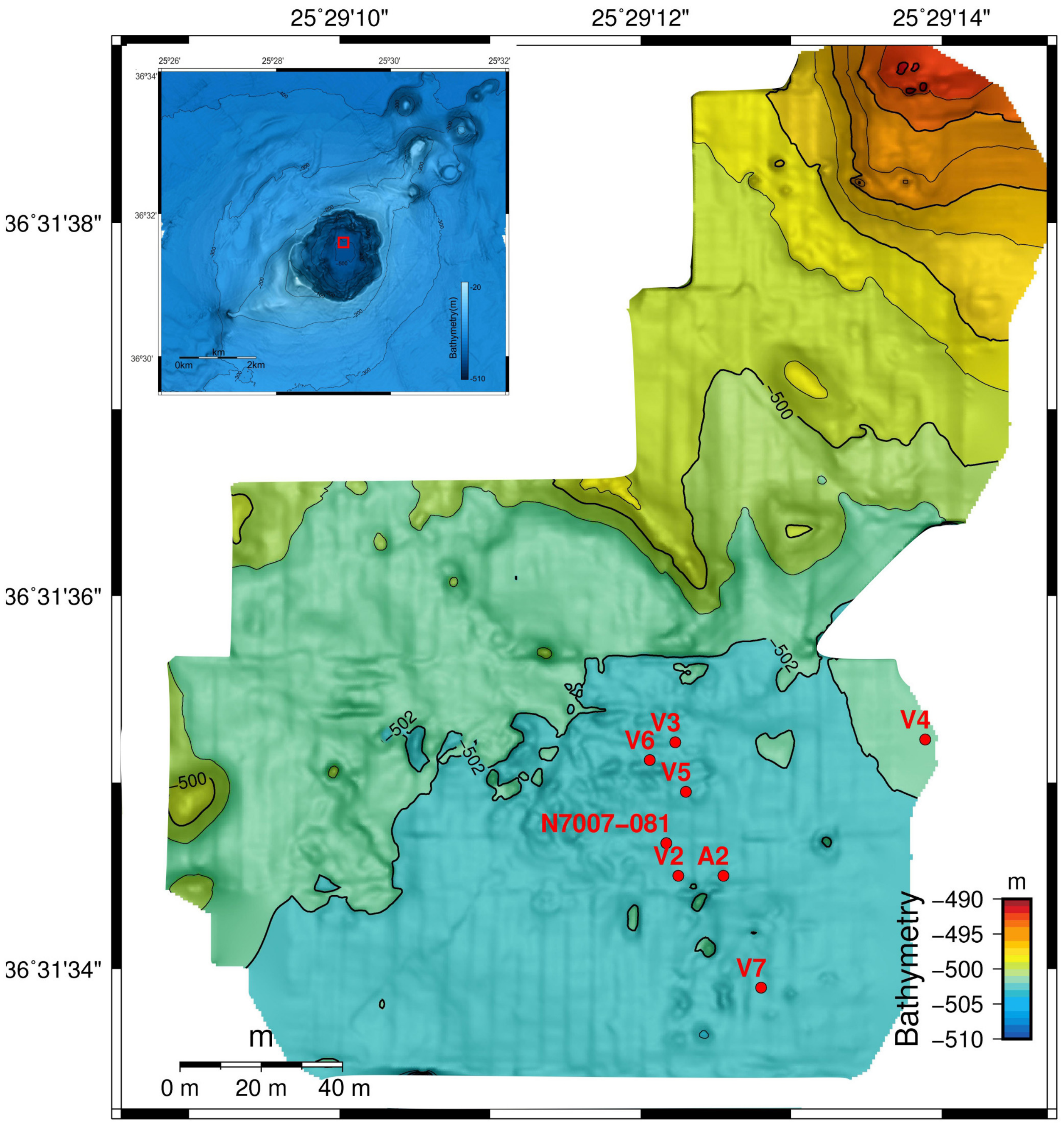

FIGURE 2 | Bathymetric map of the floor of Kolumbo submarine crater and the location of the sampled hydrothermal vents (modified after Kilias et al., 2013). Inset map shows the swathe map of Kolumbo volcano (Rizzo et al., 2016). Red rectangular indicates the location of the vent field.

These chimneys were selected based on a previous seafloor exploration of hydrothermal activity (Sigurdsson et al., 2006; Carey et al., 2013) and a oceanographic survey performed in 2014 (**Figure 2**). Although direct measurements of temperature were not possible during the 2014 survey, previous surveys found that the fluids discharged in the northern part of the crater floor had temperatures as high as 220°C, while those present along the northern and eastern margins were no hotter than 70°C, and characterized by ephemeral bubble fluxes (Sigurdsson et al., 2006; Carey et al., 2013).

The present study collected bubbling hydrothermal gases at the seafloor and stored them in titanium gas-tight bottles equipped with funnels, as described in detail by Rizzo et al. (2016). The obtained gas samples were analyzed in the laboratories of INGV (Istituto Nazionale di Geofisica e Vulcanologia), Sezione di Palermo for their chemistry and isotopic compositions of noble gases (He, Ne, and Ar), C of CO_2, and C and H of CH_4. The chemical composition of He, H_2, O_2, N_2, CO, CH_4, and CO_2 was measured by a gas chromatograph (Clarus 500, Perkin Elmer) equipped with a 3.5-m column (Carboxen 1000) and double detector (hot-wire detector and flame ionization detector [FID]), for which the analytical errors were $< 3\%$. The concentrations of C_2H_6 and C_3H_8 were also measured in a few selected samples after hydrocarbon enrichment via bubbling pressurized gas in Giggenbach bottles filled with 4-M NaOH (Giggenbach, 1975). Higher hydrocarbons were analyzed using a gas chromatograph (Shimadzu, 2010) equipped with an FID and a capillary column (CP Poraplot) using He as the carrier gas. The analytical precision for these gas chromatography analyses was better than 5% for trace gases and 10% for alkanes.

The Hg(0) concentration in the gas samples was measured at the Geosciences Environment Toulouse laboratory in France. Titanium canisters filled with hydrothermal gases at a known pressure were connected to a 60-mL impinger (Savillex) via a stainless steel valve, 6 mm of PTFE tubing and a 6-mm-long Pyrex bubbler tube. The impinger contained 30 mL of a strongly oxidizing 40 vol% inverse aqua-regia solution (HNO_3:HCl = 2:1). The canister was partly opened, which induced the hydrothermal gases to bubble in the aqua-regia solution and the oxidation of Hg(0) to Hg(II). The volume of hydrothermal gas sampled was measured with a ball flowmeter and a chronometer. The flow rate was approximately 80 mL min^{-1}, and trapping continued until atmospheric pressure equilibration occurred between the canister and the oxidizing solution trap. The total Hg concentrations were measured in accordance with the USEPA 1631 method. Aliquots of 0.1–1 mL were analyzed in duplicate using semiautomatic cold vapor atomic fluorescence spectrometry (CV-AFS; Brooks Rand Model III, United States) with a single gold trap. The analysis accuracy of CV-AFS was evaluated according to the standard analysis method for the NRC ORMS-4 certified reference material (22.0 ± 1.6 ng L^{-1}, mean ± SD), and satisfactory results were obtained (21.3 ± 2.4 ng L^{-1}, $n = 7$).

The $^{3}He/^{4}He$ and $^{4}He/^{20}Ne$ ratios addressed in the present study have been reported together with the respective analytical methods by Rizzo et al. (2016). The $^{40}Ar/^{36}Ar$ and $^{38}Ar/^{36}Ar$ ratios were measured using a mass spectrometer (Argus GVI) with analytical errors of $< 0.2\%$.

The C-isotope composition of CO_2 [expressed as $\delta^{13}C$ ‰ vs. V-PDB (Vienna-Pee Dee Belemnite)] was determined using a continuous-flow isotope-ratio mass spectrometer (Thermo Delta Plus XP, Finnigan), connected to a gas chromatograph (Trace GC) and interface (Thermo GC/C III, Finnigan). The gas chromatograph and its column (length = 30 m and i.d. = 0.32 mm; Poraplot-Q) were operated at a constant temperature of 50°C using He as the carrier gas. The analytical errors were <0.1‰. The C and H isotopes of CH_4 were analyzed using the same instrument. A combustion interface (Thermo GC III, Finnigan) was used to produce CO_2 from methane, while a gas-chromatograph/thermal-conversion interface provided on-line high-temperature conversion of CH_4 into H. The SDs for the $\delta^{13}C$ and δD measurements of CH_4 were <0.2 and <2.5‰, respectively.

RESULTS

Gas Chemistry

The chemical composition of submarine gases collected at Kolumbo is presented in **Table 1**. These gases are dominated by CO_2, which is present at concentrations up to 99.1% (**Figure 3A**). The concentration of CH_4 ranges from 1052 to 5521 ppm, while C_2H_6 and C_3H_8 exhibit much narrow ranges of 95–128 and 14–20 ppm, respectively (values measured in the Giggenbach bottle; Giggenbach, 1975). He varies between 9 and 40 ppm, while H_2 and CO range from 170 to 716 ppm and from 2 to 7 ppm, respectively. The O_2 and N_2 contents varied depending on the degree of sample contamination by ambient air, with maximum values of 5.1 and 21%, respectively (**Figures 3B**, **4A**). ^{20}Ne ranges between 0.082 and 4.2 ppm, while ^{40}Ar ranges between 69 and 834 ppm (**Figure 4B**). It should be noted that ^{40}Ar was not measured in the sample with the greatest air contamination (O_2 = 5.1%, N_2 = 21%, and ^{20}Ne = 4.2 ppm). In order to evaluate the extent of air or the presence of air-saturated water (ASW), O_2 and Ar are plotted versus ^{20}Ne in **Figures 4A,B**, respectively. All of the analyzed samples fell along the line representing air rather than ASW, indicating that this contamination is probably due to sampling or extraction procedures. In order to determine the gas composition before air contamination (G_f), data were corrected based on the O_2 content measured in each analysis as follows:

$$Gf = \frac{(Gs - (Ga \times F))}{(1 - F)}$$

where *Gs* is the concentration of the gaseous species measured in the sample (e.g., He), *Ga* is the concentration of the same gaseous species in air (e.g., He = 5.24 ppm) and *F* is the fraction of air calculated from the O_2 concentration measured in the sample divided by the atmospheric O_2 concentration (20.947%). We point out that even assuming that all of the ^{20}Ne or ^{40}Ar measured in our samples is of atmospheric origin (as for O_2), the recalculated percentages of air contamination would still be comparable. The back-corrected chemical composition of Kolumbo gases is reported in **Table 2**.

Furthermore, the concentration of gaseous Hg(0) differed markedly (and significantly) among the seven investigated chimneys, from 61 to 1301 ng m^{-3} (**Table 3**).

Isotopic Composition of Gases

Table 1 reports the isotopic compositions of CO_2, CH_4, and Ar in the analyzed gases. The C-isotope composition ($\delta^{13}C_{CO_2}$) varied between −0.04 and 1.15‰ V-PDB, whereas increasing ratios were positively correlated with the concentrations of He, H_2, CO, and CH_4. The CH_4-isotope composition varied over a narrow range for both C ($\delta^{13}C = -18.8$ to -17.6‰ V-PDB) and H ($\delta D = -118.6$ to -115.4‰ V-SMOW).

The $^{3}He/^{4}He$ and $^{4}He/^{20}Ne$ ratios used in the present study were previously measured and discussed by Rizzo et al. (2016). Here we further measured the Ar-isotope composition, which was found to be close to the values typically encountered in atmospheric air ($^{40}Ar/^{36}Ar$ = 295.5 and $^{38}Ar/^{36}Ar$ = 0.188; Ozima and Podosek, 1983). $^{40}Ar/^{36}Ar$ in hydrothermal gases varies between 296 and 316, while $^{38}Ar/^{36}Ar$ is between 0.187 and 0.189.

TABLE 1 | Chemical composition of major and minor gaseous components from Kolumbo hydrothermal vents. Ar, CO_2, and CH_4 isotope ratios are also reported.

Sample	Depth (m)	Latitude	Longitude	He (ppm)	Ne (ppm)	^{40}Ar (ppm)	^{36}Ar (ppm)	H_2 (ppm)	O_2 %	N_2 %	CO (ppm)	CH_4 (ppm)	C_2H_6 ppm	C_3H_8 ppm
A2	497	36°31.5700′ N	25°29.2110′ E	24.1	0.086	100	0.323	410.7	0.17	1.1	4.2	3270.6	95	14
V2	498	36°31.5700′ N	25°29.2050′ E	9.0	4.218	–	–	169.6	5.12	21.0	2.2	1052.2	–	–
V2	498	36°31.5700′ N	25°29.2050′ E	15.1	1.685	834	2.823	308.6	2.11	8.6	3.3	1938.6	–	–
V3	498	36°31.5843′ N	25°29.2046′ E	26.0	0.104	76	0.241	508.8	0.10	0.9	4.6	3689.1	128	18
V4	498	36°31.5846′ N	25°29.2378′ E	11.1	1.149	696	2.349	193.9	1.51	6.6	2.5	1519.4	–	–
V4	498	36°31.5846′ N	25°29.2378′ E	26.5	0.843	455	1.526	471.5	1.10	5.1	4.3	3119.2	–	–
V5	500	36°31.5790′ N	25°29.2060′ E	25.3	1.389	710	2.386	402.0	1.72	7.6	4.7	3391.8	–	–
V5	500	36°31.5790′ N	25°29.2060′ E	26.1	0.509	294	0.981	464.3	0.67	3.1	4.6	3077.5	–	–
V6	498	36°31.5824′ N	25°29.2012′ E	19.8	0.082	69	0.222	405.9	0.00	0.6	2.1	2848.2	118	20
V7	498	36°31.5580′ N	25°29.2160′ E	39.5	0.291	182	0.590	716.4	0.17	1.3	7.1	5521.5	100	15
NA007-081*	502	36°31.5735′ N	25°29.2034′ E	24.4	0.025	–	–	400.0	0.01	0.3	b.d.l.	2699.9	–	–
NA007-009*	502	36°31.6059′ N	25°29.1969′ E	–	–	–	–	299.9	0.01	0.2	b.d.l.	2598.7	–	–
ASSW				2.3	9.7	15936			34.30	62.6	0.2	3.8		
AIR				5.24	16.48	9300	31.5	0.53	20.95	78.084	0.25	1.7		

TABLE 1 | Continued

Sample	$C_1/(C_2 + C_3)$	CO_2 %	F Air	$^{40}Ar/^{36}Ar$	Err $_{40/36}$ + /−	$^{38}Ar/^{36}Ar$	Err $_{38/36}$ + /−	^{40}Ar* (ppm)	$^4He/^{40}Ar^*$	δ $^{13}C_{CO_2}$ ‰ vs. PDB	$\delta^{13}C$-CH_4 ‰ vs. PDB	δD-CH_4 ‰ vs. SMOW
A2	1817	98.4	0.0081	310.2	0.052	0.1880	0.0001	4.8	5.0	0.60	−17.6	−115.4
V2	–	73.8	0.2443	–	–	–	–	–	–	−0.04	–	–
V2	–	89.1	0.1006	296.0	0.051	0.1870	0.0001	–	–	–	–	–
V3	1699	98.6	0.0048	315.9	0.060	0.1878	0.0001	5.0	5.3	0.75	−18.8	−116
V4	–	91.7	0.0723	296.0	0.065	0.1879	0.0001	–	–	−0.03	–	–
V4	–	93.4	0.0526	298.1	0.043	0.1872	0.0001	–	–	–	–	–
V5	–	90.3	0.0820	297.4	0.051	0.1891	0.0001	–	–	0.63	–	–
V5	–	95.9	0.0321	299.3	0.065	0.1876	0.0002	–	–	0.63	–	–
V6	1964	99.1	0.0000	311.6	0.059	0.1876	0.0001	3.6	5.5	0.46	−18.1	−118.6
V7	1948	97.9	0.0082	308.9	0.069	0.1875	0.0002	8.1	4.8	1.15	–	–
NA007-081*	–	99.4	0.0005	–	–	–	–	–	–	–	–	–
NA007-009*	–	99.5	0.0005	–	–	–	–	–	–	–	–	–
ASSW		1.4	1									
AIR		0.038	1	295.5		0.188				−8		

*C_2H_6 and C_3H_8 were measured in Giggenbach bottles and then recalculated to the dry gas. *Sample from Carey et al. (2013). b.d.l., below detection limit. –, not determined.*

However, ^{40}Ar was corrected for atmospheric contamination (^{40}Ar*) in the samples having $^{40}Ar/^{36}Ar > 308$ as follows:

$$^{40}Ar^* = {}^{40}Ar_{sample} - [{}^{36}Ar_{sample} \cdot ({}^{40}Ar/{}^{36}Ar)_{air}]$$

This correction is useful for obtaining accurate estimates of the $^4He/^{40}Ar^*$ ratio, which in Kolumbo gases vary between 4.8 and 5.5. These ratios are within the ratio range typical of the mantle ($^4He/^{40}Ar = 1$–5; e.g., Ozima and Podosek, 1983; Marty, 2012), confirming that Kolumbo gases preserve the features that they have inherited from the magma.

DISCUSSION

Gas–Water Interaction of Magmatic Fluids

The chemical composition of gases corrected for air contamination as well as the $\delta^{13}C_{CO_2}$ show a variability clearly modulated by a process of selective dissolution of gases in water driven by their different solubilities (**Figures 5**, **6**). In order to determine the original composition of the intact gases, which is necessary for evaluating the origin of CO_2 and the pressure and temperature conditions of the hydrothermal system, we initially defined the boundary conditions for modeling. Due to the lack of direct measures of temperature in the fluids discharged from the Kolumbo chimneys, we assumed a homogeneous emission temperature of 220°C, as measured by Sigurdsson et al. (2006) (see section "Sampling and Analytical Techniques"). This assumption is reasonable because it is based on direct measurements made in the same part of the floor of Kolumbo submarine crater and from vents showing a sustained flux of gas bubbles, which indicates the concomitant release of high-temperature fluids (Sigurdsson et al., 2006). Regardless of the accuracy of this estimate, it should be remembered that any slight difference in temperature between vents would mostly influence the extent of the CO_2 dissolution in water rather than the path of fractionation of less-soluble species, especially when

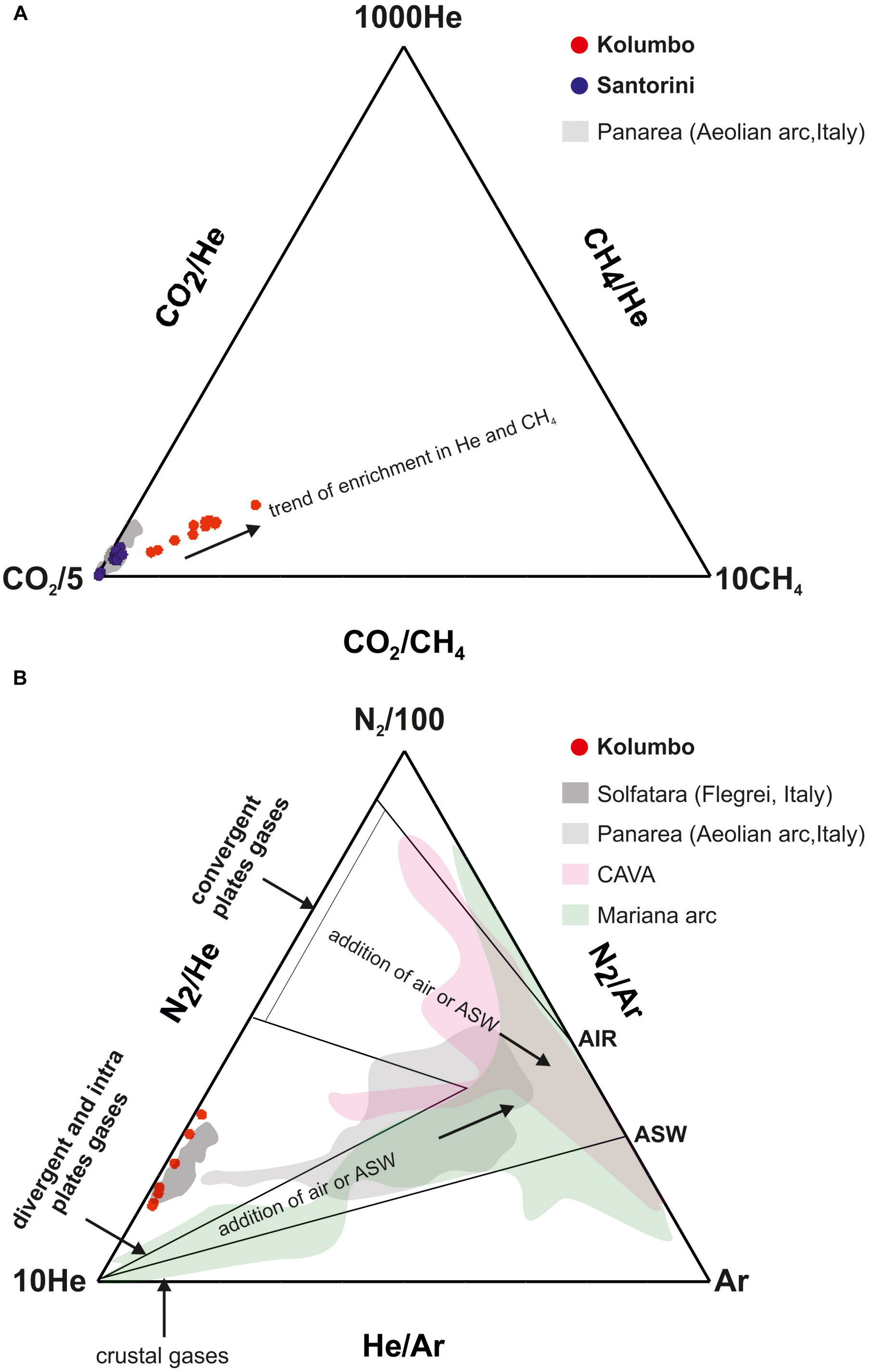

FIGURE 3 | (A) CO_2-CH_4-He ternary diagram showing the main components of Kolumbo gases. **(B)** He-Ar-N_2 ternary diagram displaying air and ASW (air-saturated water) contamination trends.

considering elemental ratios. Since gases are emitted on the floor of Kolumbo submarine crater, which is at around 500 m b.s.l., we assumed a constant pressure of 50 bar. Based on the assumption of a temperature of 220°C, the saturated vapor pressure would be ~23 bar. This means that the partial pressure of CO_2 would be ~27 bar within a bubble of fluids exsolved from the vents located at the hydrostatic pressure of 50 bar.

Considering that we are dealing with submarine emissions, it is reasonable to assume that hydrothermal water condenses in the seawater together with the highly soluble acidic gases

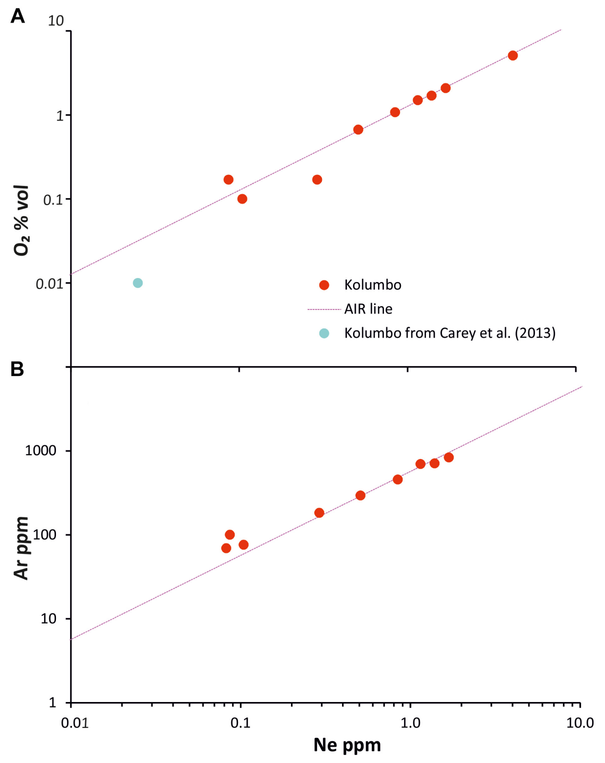

FIGURE 4 | Binary plots of Ne versus **(A)** O_2 and **(B)** Ar, with the air line also shown. Data plotting along the air line represent evidence of atmospheric contamination due to sampling or storage conditions. See the main text for details.

(SO_2, HCl, and HBr). We cannot exclude that the CO_2 continued to dissolve in water inside the gas-tight bottles during the time that lapsed between sampling and gas extraction aboard the vessel, mostly because of cooling.

The residual gas phase that we studied comprised mainly CO_2 and secondarily N_2, H_2, CO and CH_4, as well as noble gases at low levels and trace gases. We ultimately assumed a geochemical system comprising CO_2, N_2, H_2, CO, CH_4, He, Ne and Ar, all of which dissolve in liquid water according to Henry's law. After the condensation of water vapors and highly soluble acidic gases, a further progression of gas dissolution would induce the preferential dissolution of CO_2 in water and the consequent enrichment of less-soluble species such as N_2, H_2, CO, hydrocarbons and noble gases (Sander, 2015). Since our dry gas mixture comprised > 97% CO_2, we deduce that the extent of fractionation was low. Therefore, this process can be better evaluated using other components such as CH_4 versus He (**Figures 5**, **6**) rather than the CO_2 concentration.

Following the thermodynamic approach proposed by Fernandez-Prini et al. (2003 and references therein) and based on our pressure and temperature boundary conditions, we calculated Henry's constant k_H and the gas–liquid distribution constant K_D for each species included in our geochemical system. We simulated a condensation process under equilibrium conditions as expressed by the Rayleigh (1896) equation:

$$\frac{Rv}{Rv_0} = f^{\alpha - 1}$$

where Rv_0 is the initial ratio of the bulk composition (e.g., He/CO_2), Rv is the same instantaneous ratio in the residual gas phase (v), f is the fraction of the residual gas phase and α is the fractionation factor determined by the solubility ratio of the species under consideration (e.g., k_{H-He}/k_{H-CO_2}). We also assumed open-system conditions considering the continuous removal of gas-saturated parcels of water.

The initial composition applied in our model is reported in **Table 2** and in the captions of **Figures 5–7**. Similarly to gas levels, the isotopic composition of gaseous CO_2 ($\delta^{13}C_{CO_2}$) changes as a result of its dissolution in water (**Figure 7**) and the

TABLE 2 | Restored chemical composition after correction for atmospheric contamination and pristine composition of gases after correction for CO_2 dissolution in water.

Sample	Depth (m)	Latitude	Longitude	He (ppm)	H_2 (ppm)	N_2 %	CO (ppm)	CH_4 (ppm)	CO_2 %	He/CO_2	CH_4/CO_2	CO_2/^{3}He^
A2	497	36°31.5700′ N	25°29.2110′ E	24.3	414.0	0.4	4.2	3297.2	99.2	2.44E-05	3.32E-03	4.19E+09
V2	498	36°31.5700′ N	25°29.2050′ E	10.2	223.6	2.5	2.8	1387.7	97.3	1.05E-05	1.43E-03	9.78E+09
V2	498	36°31.5700′ N	25°29.2050′ E	16.2	342.8	0.8	3.7	2153.1	98.9	1.64E-05	2.18E-03	6.22E+09
V3	498	36°31.5843′ N	25°29.2046′ E	26.1	511.2	0.5	4.6	3706.7	99.0	2.64E-05	3.74E-03	3.87E+09
V4	498	36°31.5846′ N	25°29.2378′ E	11.6	208.8	1.0	2.7	1636.5	98.8	1.17E-05	1.66E-03	8.79E+09
V4	498	36°31.5846′ N	25°29.2378′ E	27.7	497.5	1.1	4.5	3290.6	98.5	2.81E-05	3.34E-03	3.63E+09
V5	500	36°31.5790′ N	25°29.2060′ E	27.0	437.5	1.3	5.1	3691.4	98.3	2.75E-05	3.76E-03	3.72E+09
V5	500	36°31.5790′ N	25°29.2060′ E	26.8	479.6	0.6	4.8	3178.7	99.0	2.71E-05	3.21E-03	3.74E+09
V6	498	36°31.5824′ N	25°29.2012′ E	19.8	405.9	0.6	2.1	2848.2	99.1	2.00E-05	2.87E-03	5.13E+09
V7	498	36°31.5580′ N	25°29.2160′ E	39.7	722.3	0.7	7.1	5566.8	98.7	403E-05	5.64E-03	2.55E+09
NA007-081*	502	36°31.5735′ N	25°29.2034′ E	24.4	400.2	0.2	–	2701.2	99.4	2.45E-05	2.72E-03	4.29E+09
NA007-009*	502	36°31.6059′ N	25°29.1969′ E	–	300.0	0.2	–	2599.9	99.5	–	2.61E-03	–
Pristine composition of gases before CO_2 dissolution in water				8	150	0.2	1.5	1150	99.8	8.02E-06	1.15E-03	1.26E+10

**Sample from Carey et al. (2013). ^^{3}He from Rizzo et al. (2016).*

TABLE 3 | Hydrothermal gas Hg(0) concentrations of the seven chimneys where it was possible to make measurements.

Sample	Depth (m)	Latitude	Longitude	Hg0 concentration (canister) (ng/m^3)
A2	497	36°31.5700′ N	25°29.2110′ E	61
V1	498	36°31.5700′ N	25°29.2050′ E	1301
V2	498	36°31.5700′ N	25°29.2050′ E	612
V3	498	36°31.5843′ N	25°29.2046′ E	153
V5	500	36°31.5790′ N	25°29.2060′ E	73
V6	498	36°31.5824′ N	25°29.2012′ E	84
V7	498	36°31.5580′ N	25°29.2160′ E	819

isotopic fractionation between gaseous and dissolved inorganic CO_2 [CO_2(aq)]. CO_2(aq) is referred to as dissolved inorganic C (DIC) and is equal to the sum of the aqueous species H_2CO_3, HCO_3^-, and CO_3^{2-}. The fractionation process is modeled using the Rayleigh equation as follows (Clark and Fritz, 1997):

$$\delta^{13}C_{CO_2} = (\delta^{13}C_{CO_2})_0 + \varepsilon \ln(f)$$

where $(\delta^{13}C_{CO_2})_0$ is the initial CO_2-isotope composition, f is the fraction of the residual gas phase, and ε is the fractionation factor between DIC and gaseous CO_2 ($CO_{2(g)}$). This fractionation factor is obtained by summing up the fractionation factors of dissolved C species and $CO_{2(g)}$ weighted for their molar fraction with respect DIC (Zhang et al., 1995; Allègre, 2008):

$$\varepsilon_{DIC-CO_2(g)} = \frac{[H_2CO_3]\varepsilon_{H_2CO_3-CO_2(g)} + [HCO_3^-]\varepsilon_{HCO_3^- - CO_2(g)} + [CO_3^{2-}]\varepsilon_{CO_3^{2-}-CO_2(g)}}{[H_2CO_3] + [HCO_3^-] + [CO_3^{2-}]}$$

The molar fraction of each C species depends on the water temperature and pH. We calculated each fractionation factor at 220°C based on the approach of Zhang et al. (1995), while the molar fractions of H_2CO_3 and HCO_3^- were set to 0.96 and 0.04, respectively. We also assumed that the molar fraction of CO_3^{2-} was 0 given that the pH of water on the floor of Kolumbo submarine crater is typically lower than 8 (Mandalakis et al., 2019), which means that the terms involving [CO_3^{2-}] can be neglected in the above equation. Under these conditions, $\varepsilon_{DIC-CO_2(g)}$ was calculated to be −0.79. The molar fractions were also used in the following equation describing the dissociation of H_2CO_3 in order to estimate the pH of water in which CO_2 was dissolved:

$$H_2CO_{3(aq)} \leftrightarrow H^+_{aq} + HCO^-_{3(aq)}$$

$$K_{A1} = \frac{[HCO_3^-][H^+]}{[H_2CO_3]} = 4.3 \cdot 10^{-7}$$

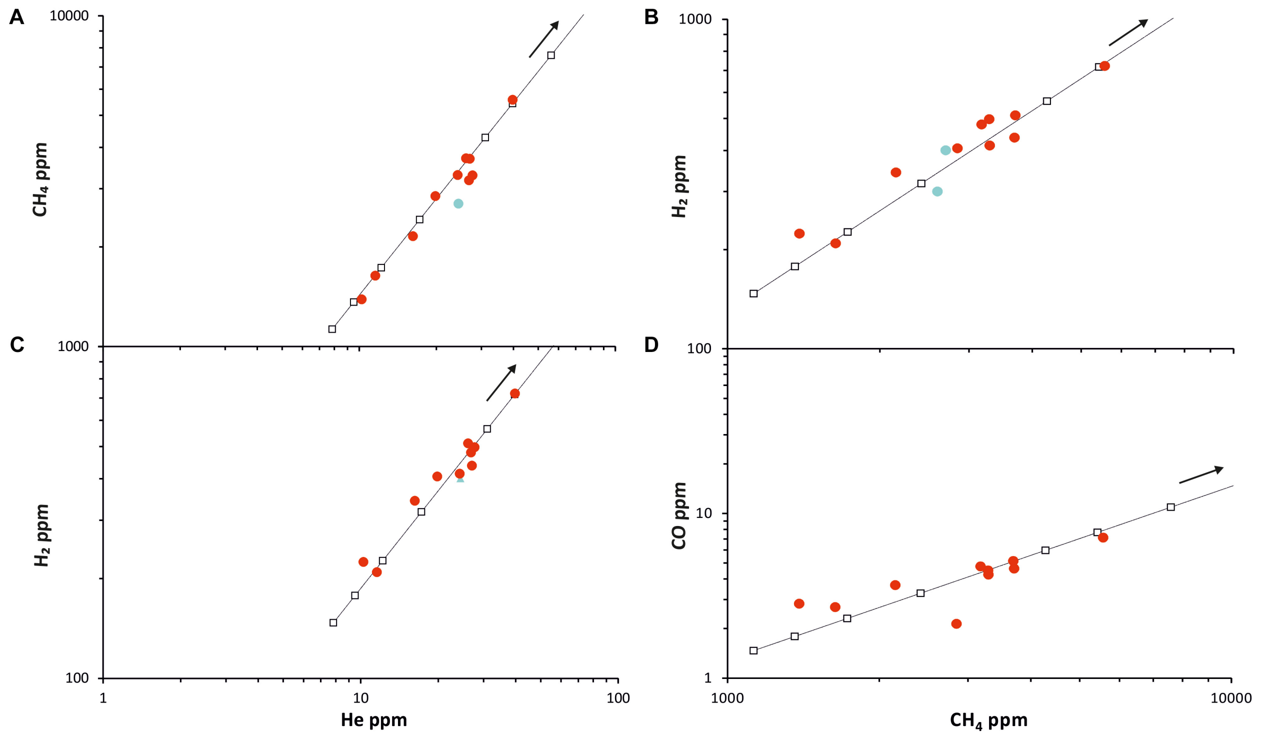

FIGURE 5 | Plots of He versus **(A)** CH_4 and **(B)** H_2, and CH_4 versus **(C)** H_2 and **(D)** CO. Legend symbols as in **Figure 4**. Lines show the path of selective dissolution of gases in water modeled as an open-system condensation process under equilibrium conditions. Arrows indicate the process direction. The starting gas composition for modeling was He = 8 ppm, H_2 = 150 ppm, N_2 = 0.2%, CH_4 = 1150 ppm, CO = 1.5 ppm and CO_2 = 99.8%. See the main text and **Table 2** for further details.

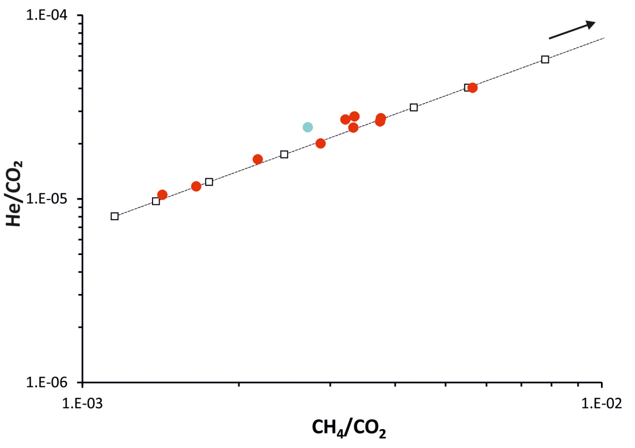

FIGURE 6 | Plot of CH_4/CO_2 versus He/CO_2. Legend symbols as in **Figure 4**. Line and arrow are as in **Figure 5**. The starting gas composition for modeling was $CH_4/CO_2 = 1.15 \times 10^{-3}$ and $He/CO_2 = 8.02 \times 10^{-6}$. See the main text for further details.

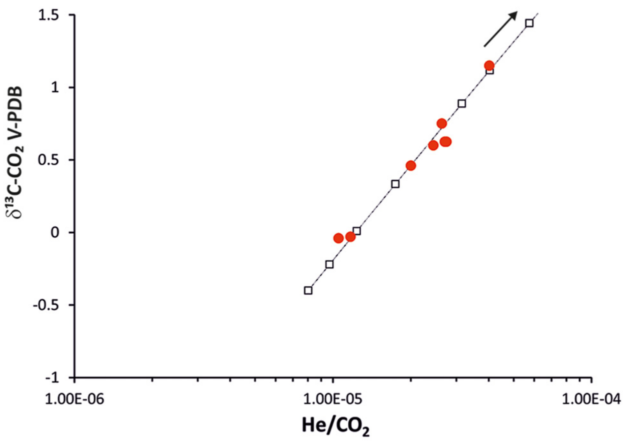

FIGURE 7 | Plot of He/CO_2 versus $\delta^{13}C_{CO_2}$. Legend symbols as in **Figure 4**. Line and arrow are as in **Figure 5**. The starting gas composition for modeling was $\delta^{13}C_{CO_2} = -0.4‰$ and $He/CO_2 = 8.02 \times 10^{-6}$. $\varepsilon_{DIC-CO_2g} = -0.79$ at 220°C, which implies H_2CO_3 and HCO_3^- molar fractions of 0.96 and 0.04, respectively, equivalent to pH = 5. See the main text for further details.

The chemical and $\delta^{13}C_{CO_2}$ variability of gases emitted from Kolumbo (**Figures 7**, **8**) is well-modeled by a trend of CO_2 dissolution in water having H_2CO_3 and HCO_3^- molar fractions of 0.96 and 0.04, respectively, which at 220°C corresponds to pH ∼5. It is particularly interesting that this value is identical to that measured by Carey et al. (2013) in fluids emitted by a neighboring vent on the floor of Kolumbo submarine crater thereby further validating the boundary conditions selected for our model.

Origin of Gases Emitted at Kolumbo

Origin of CO_2

Back-corrected calculations of the concentration and isotopic composition of gaseous CO_2 before its selective dissolution in water allow evaluation of its origin in the Kolumbo magmatic system and the making of inferences about the local mantle. To our knowledge, this is the first study to provide data on $\delta^{13}C_{CO_2}$ emitted by Kolumbo submarine volcano.

We examined the origin of CO_2 by combining the $^3He/^4He$ values reported by Rizzo et al. (2016) with the CO_2 concentration and $\delta^{13}C_{CO_2}$ values measured in the present study. The plot of $\delta^{13}C_{CO_2}$ versus $CO_2/^3He$ is a convenient diagnostic for this purpose (Sano and Marty, 1995), although post-magmatic processes may strongly modify the original gas composition and thus compromise the accuracy of this approach (e.g., Oppenheimer et al., 2014). As discussed in Section "Gas–Water Interaction of Magmatic Fluids," the trend of the variation of Kolumbo gases is modulated by the process of CO_2 dissolution in water, which can be observed in **Figure 8**. However, the back-corrected calculated values for the gas composition produced $\delta^{13}C_{CO_2}$ and $CO_2/^3He$ values of −0.4‰ and 1.28×10^{10}, respectively. This $CO_2/^3He$ ratio falls within the range of values reported for gases emitted from arc volcanoes worldwide ($\geq 10^{10}$; Hilton et al., 2002), while $\delta^{13}C_{CO_2}$ is within the range proposed for limestone ($CO_2/^3He \sim 1 \times 10^{13}$, $\delta^{13}C = -1$ to $+1‰$; Sano and Marty, 1995). **Figure 8** presents the binary mixing line between MORB ($CO_2/^3He = 2 \times 10^9$, $\delta^{13}C = -4‰$) and limestone (assuming $CO_2/^3He = 1 \times 10^{13}$, $\delta^{13}C = 0‰$), which highlights that gases emitted at Kolumbo have a MORB source contaminated by limestone. The main question arising from this evaluation is whether the contamination by carbonates occurs in the mantle (by subduction of limestone-bearing sediments) or in the crust (from carbonates in the basement). Unfortunately we have not performed any direct measurements of mantle fluids that could shed light on this question for Kolumbo, in contrast to the values measured for the mantle cumulates at Stromboli arc volcano (Gennaro et al., 2017). We therefore attempted to address this issue indirectly by comparing our data with those for fumarole gases emitted at Santorini (Nea Kameni Island) and Nisyros (**Figure 8**), which are the most-active volcanoes along HVA. Recent measurements of fumarole samples from Santorini (Rizzo et al., 2015) produced $\delta^{13}C_{CO_2}$ and $CO_2/^3He$ values that are comparable to those for Kolumbo gases, despite the considerable variability that may have been caused by gas–water interaction, similarly to our case study (**Figure 8**). In detail, $\delta^{13}C_{CO_2}$ as measured previously at Nea Kameni fumaroles was $-0.2 \pm 2.7‰$ (Dotsika et al., 2009; Parks et al., 2013; Tassi et al., 2013), which is consistent with the present results for Kolumbo (**Figure 8**). Similar $\delta^{13}C_{CO_2}$ and $CO_2/^3He$ values were also found by Brombach et al. (2003) for Nisyros fumaroles, although those data exhibited substantial variability. However, the reported range of values fell mainly within the binary mixing line between MORB and limestone, as observed for Santorini and Kolumbo gases.

Parks et al. (2013) proposed that the C-isotope signature of CO_2 emitted at Santorini and Nisyros is consistent with mixing between magmatic fluids and crustal basement limestone, the presence of which has been inferred by Nicholls (1971) and Spandler et al. (2012). This interpretation is plausible for two main reasons: (1) similar $\delta^{13}C_{CO_2}$ signatures characterize most of the Mediterranean volcanoes where there is evidence of the presence of a carbonate basement, and (2) the $\delta^{13}C_{CO_2}$ variability

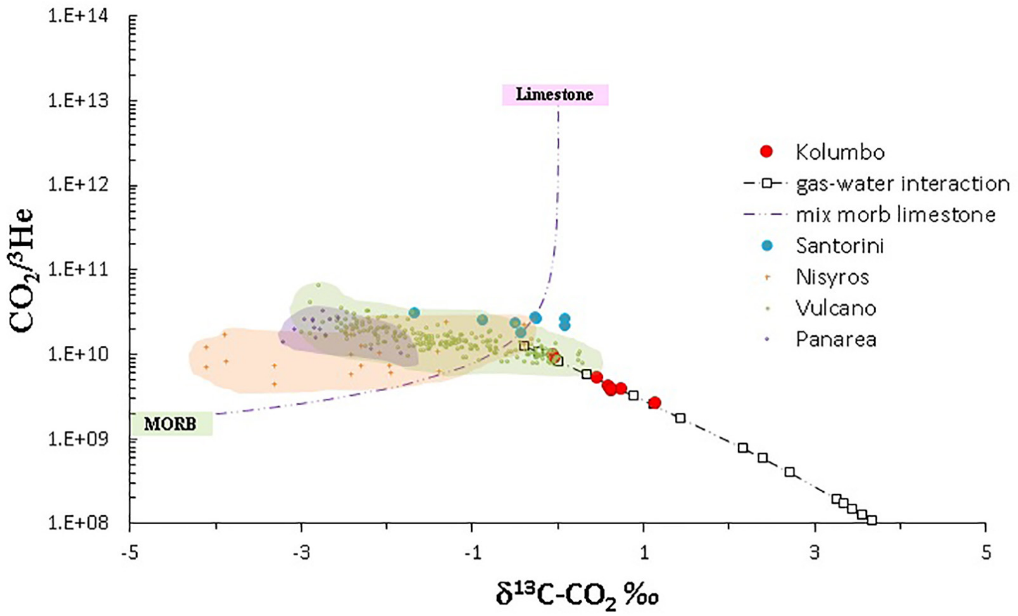

FIGURE 8 | Plot of $\delta^{13}C_{CO_2}$ versus $CO_2/^3He$. ^3He data are taken from Rizzo et al. (2016), who analyzed the same suite of gas samples. Data for Santorini, Nisyros, Vulcano, and Panarea are from Brombach et al. (2003), Paonita et al. (2013), Tassi et al. (2014), and Rizzo et al. (2015), respectively. The violet dotted curve represents binary mixing between a MORB-like upper mantle having $\delta^{13}C$ = –4‰ and $CO_2/^3He = 2 \times 10^9$, and limestone having $\delta^{13}C$ = 0‰ and $CO_2/^3He = 1 \times 10^{13}$ (Marty and Jambon, 1987; Javoy and Pineau, 1991; Sano and Marty, 1995). The black dotted line represents the path of selective dissolution of gases in water modeled by an open-system condensation process under equilibrium conditions. The starting gas composition for modeling was $\delta^{13}C_{CO_2}$ = –0.4‰ and $CO_2/^3He = 1.26 \times 10^{10}$. The symbols are as in **Figure 5**.

observed in fumaroles at Santorini during the 2011–2012 unrest (Tassi et al., 2013) is not compatible with a mantle signature modified by subducted carbonates (Parks et al., 2013). In further support of the hypothesis of Parks et al. (2013), we highlight that there is strong evidence for the presence of Mesozoic carbonates within the crust beneath Kolumbo (Kilias et al., 2013). However, Rizzo et al. (2016) reported that the $^3He/^4He$ signature of Kolumbo gases is indicative of the direct degassing of a MORB-like mantle, while those at Santorini are subsequently modified by crustal contamination. Those authors therefore argued that the mantle beneath Kolumbo and Santorini is homogeneous in terms of the He-isotope signature.

We consider that the consistency of the $\delta^{13}C_{CO_2}$ signatures at Santorini, Kolumbo, Nisyros, and most Mediterranean volcanoes with MORB and limestone mixing represents evidence of mantle metasomatism induced by decarbonation of subducting limestone-bearing sediments, rather than mixing of comparable proportions of magmatic and crustal fluids originating from local basement carbonates. Indeed, based on $\delta^{13}C_{CO_2}$ in fluid inclusions of mantle cumulates from Stromboli, Gennaro et al. (2017) revealed that the isotopic signature of local mantle reflected CO_2 contamination arising from the decarbonation of sediments carried by the subducting Ionian slab. We therefore argue that the mantle beneath Kolumbo and Santorini is reasonably homogeneous also in terms of $\delta^{13}C_{CO_2}$ signatures, and we cannot exclude that CO_2 is already contaminated by the decarbonation of slab sediments. Local crustal contamination may eventually further modify the isotopic composition of metasomatized mantle C, as observed for He isotopes beneath Santorini (Rizzo et al., 2015, 2016).

Origin of CH_4

Some studies have focused on the origin of CH_4 in fluids emitted from submarine hydrothermal systems (Welhan, 1988; McCollom and Seewald, 2007; Proskurowski et al., 2008; Keir, 2010; McDermott et al., 2015; Wen et al., 2016; Xue-Gang et al., 2016; Wang et al., 2018; and references therein). Besides the difficulty of sampling at considerable water depths, the availability of CH_4 data is further impaired by the gases emitted from hydrothermal or magmatic systems generally being dominated by CO_2 (e.g., Yang et al., 2005; Lupton et al., 2006, 2008), with only trace levels of CH_4. This compromises the ability to perform isotope analyses, especially those of H.

In this study we measured the stable C and H isotopes of CH_4 in Kolumbo hydrothermal gases and performed evaluations to ascertain the origin of CH_4. In this context we plotted $\delta^{13}C_{CH_4}$ versus $CH_4/(C_2H_6+C_3H_8)$, which is the most-common classification approach that was introduced by Bernard et al. (1978), and δD_{CH_4} versus $\delta^{13}C_{CH_4}$, as introduced by Schoell (1980) and later modified by Mazzini et al. (2011), to distinguish CH_4 originating from thermogenic and microbial processes as well as sediment-free midocean ridges (**Figure 9**). It should be stressed that the CH_4-isotope composition of Kolumbo gases (**Table 1**) varied within a narrow range for both C ($\delta^{13}C$ = −18.8 to −17.6‰ V-PDB) and H (δD = −118.6 to −115.4‰ V-SMOW). The data points in the plot of $\delta^{13}C_{CH_4}$

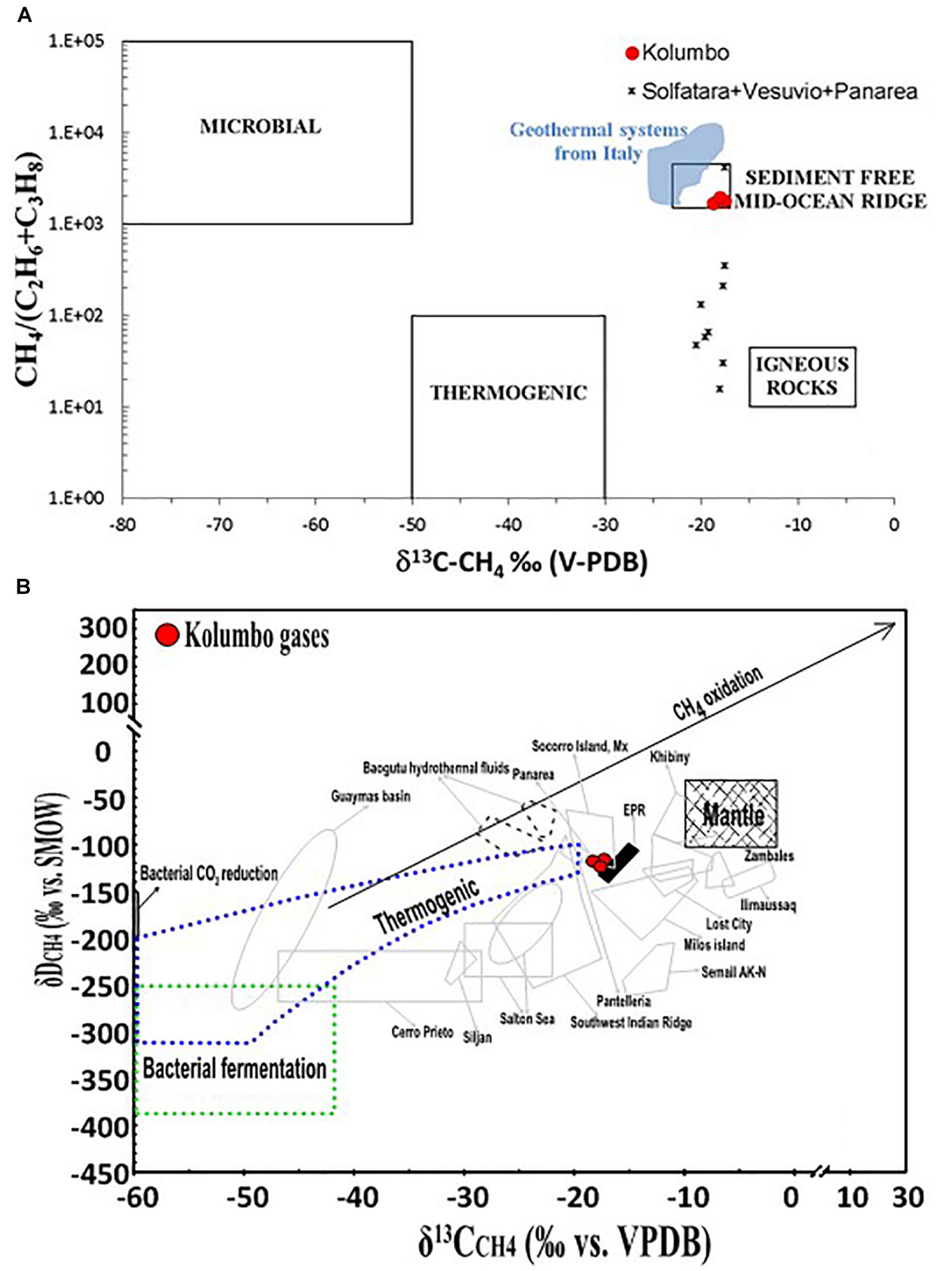

FIGURE 9 | (A) Plot of $\delta^{13}C_{CH_4}$ versus $CH_4/(C_2H_6+C_3H_8)$ modified from Bernard et al. (1978). Field data for microbial and thermogenic gases and from sediment-free midocean ridges and for igneous rocks are from McCollom and Seewald (2007 and references therein). Data for Italian geothermal systems and hydrothermal systems from Campi Flegrei, Vesuvio and Panarea are from Tassi et al. (2012 and references therein). **(B)** Plot of δD_{CH_4} versus $\delta^{13}C_{CH_4}$ as introduced by Schoell (1980) and modified by Mazzini et al. (2011). Field data are from Mazzini et al. (2011 and references therein). The symbols are as in **Figure 5**.

versus $CH_4/(C_2H_6+C_3H_8)$ for Kolumbo samples (**Figure 9A**) fall within an origin area of the sediment-free midocean ridge, similar to other Italian geothermal and hydrothermal systems (e.g., Panarea and Pantelleria; Tassi et al., 2012). Such data are often classified as abiogenic (McCollom and Seewald, 2007 and references therein), meaning that methanogenesis does not involve a biogenic organic precursor (Welhan, 1988). Nevertheless, the accuracy of this approach can be significantly compromised since the concentrations of light hydrocarbons and the isotopic composition of CH_4 can both be modified by oxidation and migration processes (Welhan, 1988). More specifically, δD_{CH_4} and $\delta^{13}C_{CH_4}$ measured in Kolumbo gases may have been altered by thermogenic gas oxidation, as in the case of CH_4 from Salton Sea Geothermal Field (Mazzini et al., 2011). Alternatively, it is possible that abiogenic CH_4 is either formed in basalts and extracted into the circulating fluids (Welhan, 1988) or produced by Fischer-Tropsch-type chemical reactions (e.g., Proskurowski et al., 2008; Keir, 2010 and references therein; Etiope and Sherwood-Lollar, 2013). However, the latter process was recently questioned by Taran et al. (2010a), who attributed the isotopic trends in the $\delta^{13}C$ and δD values of light hydrocarbons as mixing between two or more endmembers.

On the other hand, the plot of δD_{CH_4} versus $\delta^{13}C_{CH_4}$ for Kolumbo samples (**Figure 9B**) falls within the area of Socorro gases (Mexico, Taran et al., 2010b), between the range of abiotic CH_4 (McCollom and Seewald, 2007 and references therein) and a thermogenic field, which is how most geothermal and hydrothermal systems worldwide are generally characterized (Whiticar, 1999; Mango, 2000; Taran et al., 2010b; Tassi et al., 2012). By combining He-isotope data (i.e., $^3He/^4He$ ratio of ∼7 Ra for Kolumbo gases; Rizzo et al., 2016) with those of CH_4 (e.g., Hsin-Yi et al., 2016), we obtained an average $CH_4/^3He$ ratio of $\sim 1.4 \times 10^7$ (**Table 1**). This ratio falls within the range of values measured in fluids from the East Pacific Rise (e.g., Proskurowski et al., 2008; Keir, 2010; and references therein).

Christakis et al. (2018) analyzed the microbial community at Kolumbo sulfide chimneys using next-generation sequencing technologies, and did not find any microbial lineages closely related to CH_4 production processes. In addition, only a few phylotypes typically involved in CH_4 oxidation were identified. A further metagenomic investigation of the Kolumbo seafloor found negligible methanogenesis-related marker genes (Oulas et al., 2015), supporting the abiotic origin of CH_4.

It was beyond the scope of this study to resolve the scientific controversies of the different theories about abiotic CH_4. Overall, it is more likely that CH_4 in Kolumbo gases comprise a mixture of oxidized thermogenic and abiogenic CH_4 formed in high-temperature (>200°C) magmatic-hydrothermal systems.

Submarine Hydrothermal Hg(0) Emissions

The natural aerial volcanic emissions of Hg via passive degassing have been estimated at $76 \pm 30 \times 10^6$ g yr^{-1} (Bagnato et al., 2014). However, the quantity and impact of Hg released by submarine volcanoes and hydrothermal systems is less well-known due to a lack of observations (Varekamp and Buseck, 1981; Bagnato et al., 2017). In particular, there are severe logistical constraints in sampling submarine volcanic gas emissions on the floor of Kolumbo submarine crater, since it is at 500 m b.s.l. (Fitzgerald and Lamborg, 2004). Moreover, previous studies of submarine hydrothermal Hg have investigated dissolved Hg(II) concentrations but not dissolved gaseous Hg(0) (Lamborg et al., 2006).

The present study deployed gas-tight titanium syringes connected to inverted funnels above hydrothermal vents and activated by an ROV, which provided the unique opportunity to collect pristine bubbling gas emissions discharged from an active submarine volcano. The levels of gaseous Hg(0) in the gas samples varied from 61 to 1300 ng m^{-3}, which are roughly 10 times higher than the levels previously reported for on-land Santorini fumaroles (9 to 121 ng m^{-3}; Bagnato et al., 2013) and also the worldwide aerial volcanic Hg(0) concentrations (4 to 125 ng m^{-3}; Bagnato et al., 2014). These data seem to further highlight that the level of magmatic activity is higher at Kolumbo volcano than at Santorini. It is also worth mentioning that the global average concentration of atmospheric Hg(0) in the northern hemisphere is 1.5 ng m^{-3}.

Hydrothermal Gas Equilibrium

The temperature and pressure conditions at which gaseous species equilibrate in the hydrothermal system beneath the floor of Kolumbo submarine crater can be estimated from concentration data of minor reactive species together with CO_2 and H_2O (Chiodini and Marini, 1998 and references therein). The most-important assumptions in this approach are that the gaseous species have attained chemical equilibrium in the hydrothermal system and are quenched during their ascent to the sea surface. We evaluated two stability diagrams based on the concentrations of H_2, CO, CH_4, and CO_2 in the dry gas phase (**Figure 10**), following the approach proposed by Chiodini and Cioni (1989) and Chiodini et al. (2001) and subsequently modified by Chiodini et al. (2006) for submarine gases at Panarea. Because H_2O represents the main component of hydrothermal fluids, we assumed that pure water coexisted with vapor, whereas the fugacity of water vapor (fH_2O) as a function of temperature (Giggenbach, 1987) can be expressed as follows:

$$\log(fH_2O)\ (\text{bar}) = 5.510 - 2048/T$$

where T is the temperature in kelvin. It is also important to consider the fugacity of O_2 (fO_2), since this controls the redox conditions at which hydrothermal systems are formed. Since the H_2O concentration of hydrothermal vapors in our samples was not available and we have no information on the mineral assemblage that could fix fO_2, we considered the redox buffer typically proposed for hydrothermal systems by D'Amore and Panichi (1980):

$$\log(fO_2)\ (\text{bar}) = 8.20 - 23643/T$$

Complementarily, we considered the following reactions and temperature-dependent equilibrium constants based on the thermodynamic data reported by Stull et al. (1969) and Giggenbach (1980, 1987):

$$H_2O \leftrightarrow H_2 + \frac{1}{2}O_2 \qquad \log(K_{H_2O}) = 2.548 - 12707 / T$$

$$CO_2 \leftrightarrow CO + \frac{1}{2}O_2 \qquad \log(K_{CO_2}) = 5.033 - 14955 / T$$

$$CO_2 + 2H_2 \leftrightarrow CH_4 + O_2 \qquad \log(K_{CO_2+H_2}) = -4.569 - 16593 / T$$

Finally, the following equations derived by Chiodini et al. (2006) were taken into account:

$$\log(H_2/CH_4) = 8.811 - 4121.5 / T - \log(P_{CO_2})$$

$$\log(CO/CH_4) = 5.786 - 4326.5/T$$

where P is the partial pressure. The plot of $\log(CO/CH_4)$ versus $\log(H_2/CH_4)$ in **Figure 10A** suggests that Kolumbo gases would have reached an equilibrium at 200–250°C and $P_{CO_2} \sim 50$ bar. In comparison with the submarine hydrothermal system of Panarea and the high-temperature fumaroles of Vulcano (Aeolian Islands,

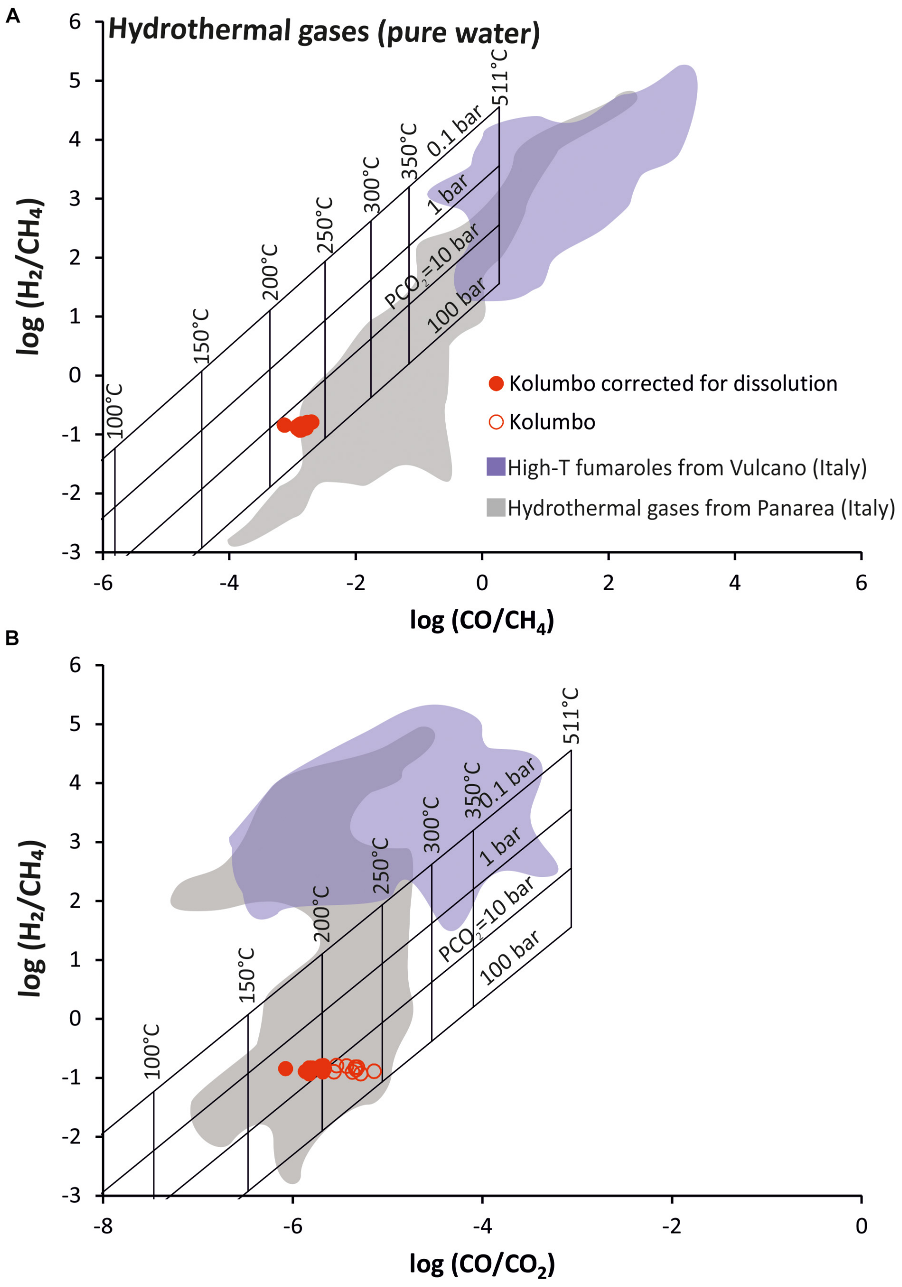

FIGURE 10 | Plots of **(A)** log(CO/CH$_4$) versus log(H$_2$/CH$_4$) and **(B)** log(CO/CO$_2$) versus log(H$_2$/CH$_4$). The theoretical grid for hydrothermal gases was calculated by assuming their coexistence with pure liquid water (Chiodini et al., 2006 and references therein). Data for Vulcano Island are from Paonita et al. (2013), and those for Panarea are from Caracausi et al. (2005), Chiodini et al. (2006), and Tassi et al. (2014). The symbols are as in **Figure 5**. See the main text for further details.

Italy), Kolumbo gases fall close to or within the range for Panarea gases, confirming their hydrothermal nature. The same pressure and temperature conditions were derived by examining the plot of log(CO/CO$_2$) versus log(H$_2$/CH$_4$) (**Figure 10B**). Given the compositional changes that may arise in hydrothermal gases due to the partial dissolution of CO$_2$ in water (see section "Gas–Water Interaction of Magmatic Fluids"), we recalculated the pressure and temperature conditions by applying the pristine composition estimated for each gas vent. Based on the values of Henry's law constant, CO$_2$ was found to differ considerably from H$_2$, CO and CH$_4$, with the former having a greater tendency to partition from the gas phase into the aqueous phase (Sander, 2015). Therefore, the correction for gas–water partitioning was deemed necessary only when considering ratios that involved CO$_2$ [e.g., log(CO/CO$_2$); **Figure 10B**]. By applying the pristine composition, we estimated a gas equilibrium temperature of

∼200°C and P_{CO_2} ∼ 10 bar. These values are slightly lower than the pressure and temperature conditions derived from the plot of $\log(CO/CH_4)$ versus $\log(H_2/CH_4)$, but they remain well within the typical values reported for hydrothermal gases. In general, the estimated temperature using CO/CH_4, CO/CO_2, and H_2/CH_4 was equal to or below the highest temperature measured on the floor of Kolumbo submarine crater vents by Sigurdsson et al. (2006) and Carey et al. (2013). This suggests that part or all of these gaseous species did not achieve equilibrium under the assumed redox conditions or that the magmatic activity has waned in recent years.

To investigate these two possibilities, we applied the approach proposed by Chiodini and Cioni (1989) and Chiodini et al. (2006), which is based on the reaction:

$$CH_4 + 3CO_2 \leftrightarrow 4CO + 2H_2O$$

Since this reaction does not involve gaseous O_2, Chiodini et al. (2006) suggested that this approach provides equilibrium pressure and temperature estimates that are independent of the redox conditions. The resulting equations that allow pressure and temperature to be determined are

$$T(K)\left[\frac{13606}{8065-\log\left(\frac{CO^4}{CO_2^3\cdot CH_4}\right)}\right]$$

$$\log P_{CO_2}(\text{bar}) = 3.573 - \frac{46}{T(K)} - \log\left(\frac{H_2}{CO}\right)$$

This specific approach revealed that Kolumbo gases equilibrated at 200–250°C and when P_{CO_2} was slightly below 50 bar (**Figure 11A**). The presence of CO_2 in one of the above equations prompted us to again consider the pristine composition of gases prior to the gas–water partitioning process. This yielded a slightly lower equilibrium temperature (189–216°C), whereas P_{CO_2} remained the same (**Figure 11A**). This temperature range is comparable to those estimated using CO/CH_4, CO/CO_2 and H_2/CH_4 ratios, suggesting that the assumed redox conditions are not responsible for the difference in the estimated equilibrium temperatures.

The findings of previous investigations of crater fumaroles at White Island (Giggenbach, 1987) and Vulcano (Chiodini et al., 1993, 1995) suggest that the two most-reactive gaseous species in hydrothermal systems are H_2 and CO, while CH_4 is one of the least reactive (Giggenbach, 1991; Taran and Giggenbach, 2003). To evaluate if CH_4 measured in Kolumbo gases attained full equilibrium, we considered the following formation reaction and relative equilibrium constant:

$$CO_2 + H_2 \leftrightarrow CO + H_2O$$

$$\log(K_{CO_2+H_2}) = \log(CO/CO_2) - \log(H_2/H_2O)$$

In the gas phase, $\log(K_{CO_2+H_2}) = -2248 / T + 2.485$

In a single saturated liquid phase, as assumed in our case, gas equilibrium contents are computed using the vapor–liquid distribution coefficient (*B*) (Giggenbach, 1980; D'Amore and Truesdell, 1988; Chiodini and Marini, 1998):

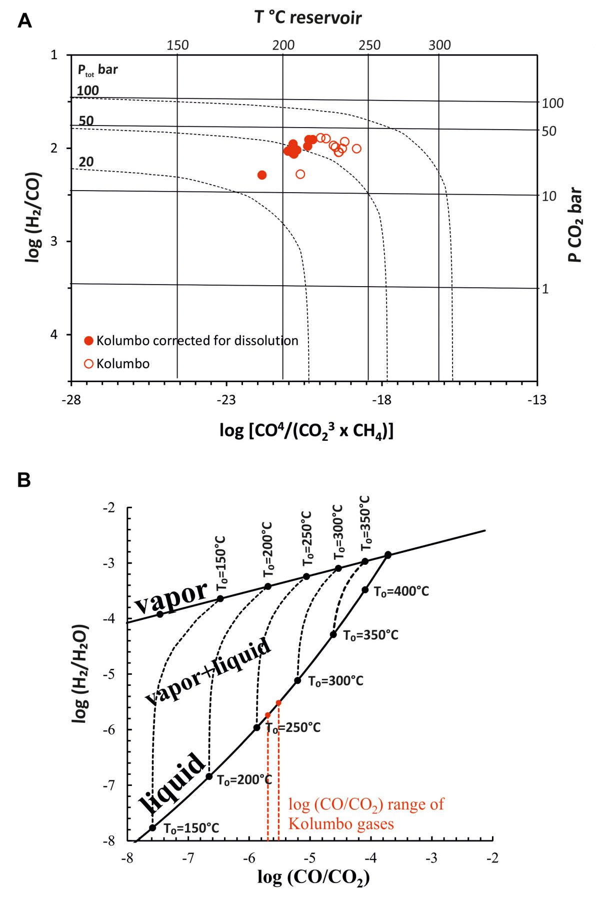

FIGURE 11 | (A) Plot of $\log[CO^4/(CO_2^3 \cdot CH_4)]$ versus $\log(H_2/CO)$. The theoretical grid refers to vapor–liquid equilibrium conditions (Chiodini et al., 2006 and references therein). **(B)** Plot of $\log(CO/CO_2)$ versus $\log(H_2/H_2O)$ following the approach proposed by Chiodini and Marini (1998). The composition of liquid, vapor and vapor separated from liquid (single-step) phases are reported assuming that the fO_2 buffer proposed for hydrothermal systems by D'Amore and Panichi (1980) controls the redox conditions. Red dotted lines indicate the range of $\log(CO/CO_2)$ for Kolumbo gases corrected for the selective dissolution of CO_2 in water. See the main text and Chiodini and Marini (1998) for further details.

$$\log(B_{CO}) = 6.3173 - 0.01388\,(T - 273.15)$$

$$\log(B_{CO_2}) = 4.7593 - 0.01092\,(T - 273.15)$$

$$\log(B_{H_2}) = 6.2283 - 0.01403\,(T - 273.15)$$

Therefore, the above reported reaction for the liquid phase becomes

$$\log(K_{CO_2+H_2}) - \log(B_{CO}/B_{CO_2}) + \log(B_{H_2}) = \log(CO/CO_2) - \log(H_2/H_2O)$$

An equilibrium temperature of 250–300°C and $\log(K_{CO_2+H_2}) - \log(B_{CO}/B_{CO_2}) + \log(B_{H_2}) \approx 0.0 \pm 0.1$ implies $\log(H_2/H_2O) \approx \log(CO/CO_2)$. Thus, the $\log(CO/CO_2)$ values measured in our

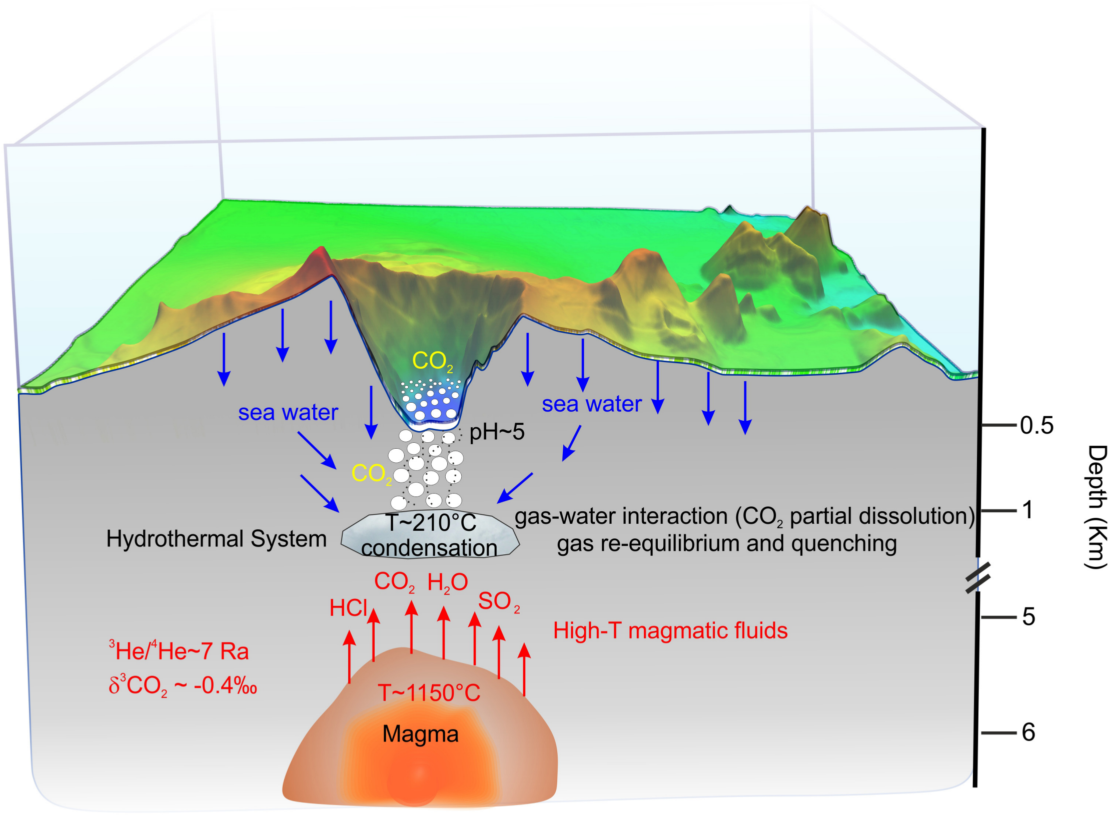

FIGURE 12 | Conceptual scheme of the hydrothermal system beneath Kolumbo. The location of the shallow magma chamber at 5–7 km beneath Kolumbo is from Dimitriadis et al. (2010), Konstantinou and Yeh (2012), and Cantner et al. (2014). The He-isotope composition is from Rizzo et al. (2016).

samples and corrected for CO_2 dissolution can be used to roughly estimate the equilibrium temperature in liquid water, which varies in the narrow range of 263–276°C (**Figure 11B**). These values are higher than those previously calculated including CH_4, and thus we deduce that the latter species was not in equilibrium with the other gases and led to underestimations of the equilibrium temperature.

Based on the relationships proposed by Chiodini and Cioni (1989), we can finally calculate $P_{CO_2} \sim 30$ bar and $P_{H_2O} \sim 36$ bar, which sum to a total pressure of ~66 bar. Considering that Kolumbo gases are emitted at 500 m b.s.l., which corresponds to a pressure of ~50 bar, the hydrothermal system must be located at a pressure of ~116 bar (~1000 m b.s.l.).

Conceptual Scheme of the Hydrothermal System Beneath Kolumbo

Based on this study and other previous findings (Sigurdsson et al., 2006; Carey et al., 2013; Kilias et al., 2013; Rizzo et al., 2016), in **Figure 12** we propose a physical and geochemical model for the Kolumbo magmatic-hydrothermal system. We made some assumptions in order to simplify the system: (1) the permeability of the system was considered uniform, isotropic and sufficiently high; (2) the shallow magma chamber located 5–7 km beneath Kolumbo (Dimitriadis et al., 2010; Konstantinou and Yeh, 2012; Cantner et al., 2014) represents the source of magmatic gases feeding the hydrothermal system, (3) magmatic degassing does not or only weakly modifies these magmatic gases, and (4) seawater infiltrates from the sea bottom and favors condensation of magmatic gases both within and above the hydrothermal system.

At Kolumbo, magmatic gases (H_2O, CO_2, S-bearing species, halogens and noble gases) having $^3He/^4He \sim 7$ Ra (Rizzo et al., 2016) and $\delta^{13}C_{CO_2} \sim -0.4‰$ ascend from the magma chamber and feed conduits up to the hydrothermal system (**Figure 12**). During the cooling of magmatic gases, H_2O and more-acidic species (S and halogens) condensate to form a hydrothermal system at ~270°C in which water at pH $\leq$ 5 probably circulates. We cannot exclude that the hydrothermal system has multiple levels; however, we are able to reconstruct the upper level that feeds the bottom vents of the crater. Hydrothermal waters are probably fed by seawater infiltrating from the sea bottom and any brine formed from the adsorption of acidic gases in groundwater by rock dissolution.

The hydrothermal system has a total pressure of ~66 bar, corresponding to ~1,160 m b.s.l. and 650 m below the crater bottom, if the hydrostatic pressure is assumed at depth. Hydrothermal gases within the hydrothermal system undergo gas–water interactions along the fractures feeding the floor of

Kolumbo submarine crater and from the shallow vents that favor the removal of most of the acidic gases (S and halogens) and the partial dissolution of CO_2 (see section "Gas–Water Interaction of Magmatic Fluids"). This produces an excess of N_2, noble gases and reactive gases via migration paths that permit their rapid ascent under advective degassing. At the crater bottom, several vents discharge fluids at temperatures up to 220°C, variable gas fluxes and pH down to ~5 (Sigurdsson et al., 2006; Carey et al., 2013). Acoustic and visual imaging of the ascending bubbles suggests that CO_2 is being dissolved into seawater within ~10 m above the crater floor (Carey et al., 2013).

CONCLUSIONS

We have investigated the geochemistry of CO_2-rich gases venting at 500 m b.s.l. from Kolumbo submarine volcano, which is located 7 km northeast of Santorini Island. The main findings are as follows:

- Gases are dominated by CO_2 (>97%), with a small air contamination probably related to sampling conditions, but are fractionated by a process of gas–water interaction reasonably related to variable fluxes of gases emitted from the different vents. This process induces a partial dissolution of gaseous CO_2 in water, leading to substantial enrichment of the residual gas in those species that are much less soluble in water (i.e., He, H_2, CO, CH_4, and N_2). This fractionation also affects the C-isotope composition of CO_2.
- We modeled the gas–water interaction process (~220°C, ~50 bar and pH ~ 5) and reconstructed the chemistry and $\delta^{13}C_{CO_2}$ of magmatic gases before interaction. We assess that the pristine CO_2 is characterized by $\delta^{13}C \sim -0.4‰$. Combining our data with $^3He/^4He$ measurements carried out in the same gas samples by Rizzo et al. (2016) yields $CO_2/^3He \sim 1 \times 10^{10}$. These data are in the same range as those obtained for the Santorini and Nisyros fumaroles. We argue that CO_2 emitted at Kolumbo could originate from a mantle contaminated by CO_2 via the decarbonation of subducting limestone.
- The CH_4-isotope composition falls within the range typical of hydrothermal gases, similar to other Mediterranean hydrothermal systems (Panarea and Campi Flegrei), suggesting that it originates from mixing between thermogenic and abiotic CH_4.
- We found that the Hg(0) concentration in Kolumbo gases ranges from ~60 to 1300 ng m^{-3}. These levels are particularly high when compared to those of land-based fumaroles located on Santorini Island and worldwide aerial volcanic emissions, which suggests that the magmatic activity is higher at Kolumbo than at Santorini.
- Based on geo-indicators of pressure and temperature, we calculated that magmatic gases equilibrate within the Kolumbo hydrothermal system at about 270°C and 116 bar.

AUTHOR CONTRIBUTIONS

AR and PN conceived the study. AR, VC, PN, PP, MM, GK, AM, and AlC participated in the collection of gas samples. AR, VC, and AnC analyzed the gas samples and elaborated the data. DL helped in figures preparation. All of the authors contributed to the preparation and editing of the final manuscript.

FUNDING

The authors acknowledge financial support from the SeaBioTech project (spider.science.strath.ac.uk/seabiotech/) funded by the European Commission within its FP7 Programme (Grant No. 311932), as well as from INGV, Sezione di Palermo, which permitted the access to analytical facilities.

ACKNOWLEDGMENTS

We thank Giuseppe Riccobono and Paolo Cosenza for providing technical support to the project and constructing the gas-tight sampler at INGV, Sezione di Palermo that was used to collect some of the submarine fluid samples. The officers and crew of RV AEGAEO are especially acknowledged for their valuable help during sampling. We thank INGV, Sezione di Palermo for providing analytical support, particularly Francesco Salerno and Mauro Martelli for performing analyses of gases chemistry, and Mariano Tantillo for supporting the laboratory activities involving noble-gas isotopes. We also thank Fausto Grassa, Giorgio Capasso, Ygor Oliveri, and Aldo Sollami for their help with the analyses of CO_2 and CH_4 isotopes in the stable-isotope laboratory. We further thank Cinzia Federico and Fausto Grassa for useful discussions that helped in the elaborative and interpretative framework. Data reported in **Tables 1–3** are available by contacting the corresponding author. We thank the Chief Editor VA the Guest Associate Editor GG for handling and revising the manuscript, YT and an reviewer for suggestions that greatly improved the manuscript. English Science Editing revised the use of English in the manuscript.

REFERENCES

Allègre, C. J. (2008). *Isotope Geology*. Cambridge: Cambridge University Press, 512. doi: 10.1017/CBO9780511809323

Bagnato, E., Acquavita, A., Barra, M., Covelli, S., Italiano, F., Oliveri, E., et al. (2017). Hydrochemical and atmochemical mercury distribution over the submarine hydrothermal hot-spot sources of Panarea Island, Aeolian Archipelago. *Mar. Chem.* 194, 63–78. doi: 10.1016/j.marchem.2017.04.003

Bagnato, E., Tamburello, G., Aiuppa, A., Sprovieri, M., Vougioukalakis, G. E., and Parks, M. (2013). Nea Kameni volcanic centre, Santorini (Greece). *Geochem. J.* 47, 437–450. doi: 10.2343/geochemj.2.0263

Bagnato, E., Tamburello, G., Avard, G., Martinez-Cruz, M., Enrico, M., Fu, X., et al. (2014). Mercury Fluxes from volcanic and geothermal sources: an update. *Geol. Soc.* 410, 263–285. doi: 10.1144/SP410.2

Bernard, B. B., Brooks, J. M., and Sackett, W. M. (1978). "A geochemical model for characterization of hydrocarbon gas sources in marine sediments," in *Proceedings of the Offshore Technology Conference*, Houston, TX, 435–438.

Bohnhoff, M., Rische, M., Meier, T., Becker, D., Stavrakakis, G., and Harjes, H.-P. (2006). Microseismic activity in the Hellenic Volcanic Arc, Greece, with emphasis on the seismotectonic setting of the Santorini–Amorgos zone. *Tectonophysics* 423, 17–33. doi: 10.1016/j.tecto.2006.03.024

Brombach, T., Caliro, S., Chiodini, G., Fiebig, J., Hunziker, J., and Raco, B. (2003). Geochemical evidence for mixing of magmatic fluids with seawater, Nisyros hydrothermal system, Greece. *Bull. Volcanol.* 65, 505–516. doi: 10.1007/s00445-003-0278-x

Butterfield, D. A., Massoth, G. J., McDuff, R. E., Lupton, J. E., and Lilley, M. D. (1990). Geochemistry of hydrothermal fluids from Axial Seamount Hydrothermal Emissions Study Vent Field, Juan de Fuca Ridge: subseafloor boiling and subsequent fluid-rock interaction. *J. Geophys. Res.* 95, 12,895–12,921.. doi: 10.1029/JB095iB08p12895

Caliro, S., Caracausi, A., Chiodini, G., Ditta, M., Italiano, F., Longo, M., et al. (2004). Evidence of a recent input ofmagmatic gases into the quiescent volcanic edifice of Panarea, Aeolian Islands, Italy. *Geophys. Res. Lett.* 31:L07619. doi: 10.1029/2003GL019359

Camilli, R., Nomikou, P., Escartín, J., Ridao, P., Mallios, A., Kilias, S. P., et al. (2015). The kallisti limnes, carbon dioxide-accumulating subsea pools. *Sci. Rep.* 5:12152. doi: 10.1038/srep12152

Cantner, K., Carey, S., and Nomikou, P. (2014). Integrated volcanologic and petrologic analysis of the 1650AD eruption of Kolumbo submarine volcano, Greece. *J. Volcanol. Geothermal Res.* 269, 28–43. doi: 10.1016/j.jvolgeores.2013.10.004

Capaccioni, B., Tassi, F., Vaselli, O., Tedesco, D., and Poreda, R. (2007). Submarine gas burst at Panarea Island (southern Italy) on 3 November 2002: a magmatic versus hydrothermal episode. *J. Geophys. Res.* 112:B05201. doi: 10.1029/2006JB004359

Caracausi, A., Ditta, M., Italiano, F., Longo, M., Nuccio, P. M., Paonita, A., et al. (2005). Changes in fluid geochemistry and physico-chemical conditions of geothermal systems caused by magmatic input: the recent abrupt outgassing off the island of Panarea, Aeolian Islands, Italy. *Geochim. Cosmochim. Acta* 69, 3045–3059. doi: 10.1016/j.gca.2005.02.011

Carey, S., Nomikou, P., Bell, K. C., Lilley, M., Lupton, J., Roman, C., et al. (2013). CO_2 degassing from hydrothermal vents at Kolumbo submarine volcano, Greece, and the accumulation of acidic crater water. *Geology* 41, 1035–1038. doi: 10.1130/G34286.1

Chiodini, G., Caliro, S., Caramanna, G., Granieri, D., Minopoli, C., Moretti, R., et al. (2006). Geochemistry of the submarine gaseous emissions of Panarea (Aeolian Islands, southern Italy): magmatic vs. hydrothermal origin and implications for volcanic surveillance. *Pure Appl. Geophys.* 163, 759–780. doi: 10.1007/s00024-006-0037-y

Chiodini, G., and Cioni, R. (1989). Gas geobarometry for hydrothermal systems and its application to some Italian geothermal areas. *Appl. Geochem.* 4, 465–472. doi: 10.1016/0883-2927(89)90004-8

Chiodini, G., Cioni, R., and Marini, L. (1993). Reactions governing the chemistry of crater fumaroles from Vulcano Island, Italy, and implications for volcanic surveillance. *Appl. Geochem.* 8, 357–371. doi: 10.1016/0883-2927(93)90004-Z

Chiodini, G., Cioni, R., Marini, L., and Panichi, C. (1995). Origin of the fumarolic fluids of Vulcano Island, Italy, and implications for volcanic surveillance. *Bull. Volcanol.* 57, 99–110. doi: 10.1007/BF00301400

Chiodini, G., and Marini, L. (1998). Hydrothermal gas equilibria: the H_2O–H_2–CO_2–CO–CH_4 system. *Geochim. Cosmochim. Acta* 62, 2673–2687. doi: 10.1016/S0016-7037(98)00181-1

Chiodini, G., Marini, L., and Russo, M. (2001). Geochemical evidence for the existence of hightemperature brines at Vesuvio volcano, Italy. *Geochem. Cosm. Acta* 65, 2129–2147. doi: 10.1016/S0016-7037(01)00583-X

Christakis, C., Polymenakou, P., Mandalakis, M., Nomikou, P., Kristoffersen, J. B., Lampridou, D., et al. (2018). Microbial community differentiation between active and inactiove sulfide chimneys of the Kolumbo submarine volcano. Hellenic Volcanic Arc. *Extremophiles* 22, 13–27. doi: 10.1007/s00792-017-0971-x

Clark, I. D., and Fritz, P. (1997). *Environmental Isotopes in Hydrogeology*. Boca Raton, FL: CRC Press, 328.

Crisp, J. A. (1984). Rates of magma emplacement and volcanic output. *J. Volcanol. Geotherm. Res.* 20, 177–211. doi: 10.1016/0377-0273(84)90039-8

D'Amore, F., and Panichi, C. (1980). Evaluation of deep temperature of hydrothermal systems by a new gasgeothermometer. *Geochim. Cosmochim. Acta* 44, 549–556. doi: 10.1016/0016-7037(80)90051-4

D'Amore, F., and Truesdell, A. H. (1988). A review of solubilities and equilibrium constants of chemical reactions for gaseous species of geothermal interest. *Sci. Geol. Bull.* 41, 309–332. doi: 10.3406/sgeol.1988.1801

Dimitriadis, I., Karagianni, E., Panagiotopoulos, D., Papazachos, C., Hatzidimitriou, P., Bohnhoff, M., et al. (2009). Seismicity and active tectonics at Coloumbo Reef (Aegean Sea, Greece): monitoring an active volcano at Santorini Volcanic Center using a temporary seismic network. *Tectonophysics* 465, 136–149. doi: 10.1016/j.tecto.2008.11.005

Dimitriadis, I., Papazachos, C., Panagiotopoulos, D., Hatzidimitriou, P., Bohnhoff, M., Rische, M., et al. (2010). P and S velocity structures of the Santorini–Coloumbo volcanic system (Aegean Sea, Greece) obtained by non-linear inversion of travel times and its tectonic implications. *J. Volcanol. Geothermal Res.* 195, 13–30. doi: 10.1016/j.jvolgeores.2010.05.013

Dotsika, E., Poutoukis, D., Michelot, J. L., and Raco, B. (2009). Natural tracers for identifying the origin of the thermal fluids emerging along the Aegean volcanic arc (Greece): evidence of arc-type magmatic water (ATMW) participation. *J. Volcanol. Geotherm. Res.* 179, 19–32. doi: 10.1016/j.jvolgeores.2008.09.024

Etiope, G., and Sherwood-Lollar, B. (2013). Abiotic methane on Earth. *Rev. Geophys.* 51, 276–299. doi: 10.1002/rog.20011

Fernandez-Prini, R., Alvarez, J. L., and Harvey, A. H. (2003). Henry's constants and vapor–liquid distribution constants for gaseous solutes in H_2O and D_2O at high temperatures. *J. Phys. Chem. Ref. Data* 32:903. doi: 10.1063/1.1564818

Fitzgerald, W. F., and Lamborg, C. H. (2004). "Geochemistry of mercury in the environment," in *Treatise on Geochemistrys: Environmental Geochemistry*, Vol. 9, ed. B. S. Lollar (New York, NY: Elsevier, Inc).

Francalanci, L., Vougioukalakis, G. E., Perini, G., and Manetti, P. A. (2005). "West-East traverse along the magmatism of the South Aegean volcanic arc in the light of volcanological, chemical and isotope data. Developments in Volcanology (Amsterdam, Olanda)," in *The South Aegean Active Volcanic Arc, Present Knowledge and Future Perspectives, 7*, eds M. Fitykas and G. E. Vougioukalakis (Amsterdam: Elsevier), 65–111. doi: 10.1016/S1871-644X(05)80033-6

Gennaro, M. E., Grassa, F., Martelli, M., Renzulli, A., and Rizzo, A. L. (2017). Carbon isotope composition of CO_2-rich inclusions in cumulate-forming mantle minerals from Stromboli volcano (Italy). *J. Volcanol. Geotherm. Res.* 346, 95–103. doi: 10.1016/j.jvolgeores.2017.04.001

Giggenbach, W. F. (1975). A simple method for the collection and analysis of volcanic gas samples. *Bull. Volcanol.* 39, 132–145. doi: 10.1007/BF02596953

Giggenbach, W. F. (1980). Geothermal gas equilibria. *Geochim. Cosmochim. Acta* 44, 2021–2032. doi: 10.1016/0016-7037(80)90200-8

Giggenbach, W. F. (1987). Redox processes governing the chemistry of fumarolic gas discharges from White Island, New Zeland. *Appl. Geochem.* 2, 143–161. doi: 10.1016/0883-2927(87)90030-8

Giggenbach, W. F., (1991). "Geothermometry," in *Isotopic and Chemical Techniques in Geothermal Exploration, Development and Use*, ed. S. Arnórsson (Vienna: International Atomic Agency), 119–142.

Hilton, D. R., Fisher, T. P., and Marty, B. (2002). Noble gases and volatile recycling at subduction zones. *Rev. Mineral. Geochem.* 47, 319–370. doi: 10.2138/rmg.2002.47.9

Hooft, E. E. E., Nomikou, P., Toomey, D. R., Lampridou, D., Getz, C., Christopoulou, M.-E., et al. (2017). Backarc tectonism, volcanism, and mass wasting shape seafloor morphology in the Santorini-Christiana-Amorgos region of the Hellenic Volcanic Arc. *Tectonophysics* 71, 396–414. doi: 10.1016/j.tecto.2017.06.005

Hsin-Yi, W., Yuji, S., Naoto, T., Yama, T., Akizumi, I., Kentaro, T., et al. (2016). Helium and methane sources and fluxes of shallow submarine hydrothermal plumes near the Tokara Islands, Southern Japan. *Sci. Rep.* 6:34126. doi: 10.1038/srep34126

Hubscher, C., Ruhnau, M., and Nomikou, P. (2015). Volcano-tectonic evolution of the polygenetic Kolumbo submarine volcano/Santorini (Aegean Sea). *J. Volcanol. Geothermal Res.* 291, 101–111. doi: 10.1016/j.jvolgeores.2014.12.020

Javoy, M., and Pineau, F. (1991). The volatiles record of a "popping" rock from the mid-Atlantic ridge at 14N: chemical and isotopic composition of gas trapped in the vesicles. *Earth Planet. Sci. Lett.* 107, 598–611. doi: 10.1016/0012-821X(91)90104-P

Keir, R. (2010). A note on the fluxes of abiogenic methane and hydrogen from mid-ocean ridges. *Geophys. Res. Lett* 37:L24609. doi: 10.1029/2010GL045362

Kilias, S. P., Nomikou, P., Papanikolaou, D., Polymenakou, P. N., Godelitsas, A., Argyraki, A., et al. (2013). New insights into hydrothermal vent processes in the unique shallowsubmarine arc-volcano, Kolumbo (Santorini), Greece. *Sci. Rep.* 3:2421. doi: 10.1038/srep02421

Klaver, M., Carey, S., Nomikou, P., Smet, I., Godelitsas, A., and Vroon, P. (2016). A distinct source and differentiation history for Kolumbo submarine volcano, Santorini volcanic field, Aegean arc. *Geochem. Geophys. Geosyst.* 17, 3254–3273. doi: 10.1002/2016GC006398

Konstantinou, K. I., and Yeh, T.-Y. (2012). Stress field around the Coloumbo magma chamber, southern Aegean: Its significance for assessing volcanic and seismic hazard in Santorini. *J. Geodyn.* 54, 13–20. doi: 10.1016/j.jog.2011.09.003

Lamborg, C. H., Von Damm, K. L., Fitzgerald, W. F., Hammerschmidt, C. R., and Zierenberg, R. (2006). Mercury and monomethylmercury in fluids from Sea Cliff submarine hydrothermal field. *Gorda Ridge Geophys. Res. Lett.* 33:L17606. doi: 10.1029/2006GL026321

Lan, T. F., Sano, Y., Yang, T. F., Takahata, N., Shirai, K., and Pinti, D. (2010). Evaluating Earth degassing in subduction zones by measuring helium fluxes from the ocean floor. *Earth Planet. Sci. Lett.* 289, 317–322. doi: 10.1016/j.epsl.2010.07.049

Le Pichon, X., and Angelier, J., (1979). The hellenic arc and trench system: a key to the neotectonic evolution of the eastern Mediterranean area. *Tectonophysics* 60, 1–42. doi: 10.1016/0040-1951(79)90131-8

Lilley, M. D., Butterfield, D. A., Olson, E. J., Lupton, J. E., Macko, S. A., and McDuff, R. E. (1993). Anomalous CH_4 and NH4+ concentrations at an unsedimented mid-ocean-ridge hydrothermal system. *Nature* 364, 45–47. doi: 10.1038/364045a0

Lupton, J., Butterfield, D., Lilley, M., Evans, L., Ko-ichi, N., Chadwick, W., et al. (2006). Submarine venting of liquid carbon dioxide on a Mariana Arc volcano. *Geochem. Geophys. Geosyst*. 7:Q08007. doi: 10.1029/2005GC001152

Lupton, J., Lilley, M., Butterfield, D., Evans, L., Embley, R., Massoth, G., et al. (2008). Venting of a separate CO_2-rich gas phase from submarine arc volcanoes: examples from the Mariana and Tonga-Kermadec arcs. *J. Geophys. Res.* 113, B08S12. doi: 10.1029/2007JB005467

Lupton, J. D., Lilley, B. M., Ishibashi, J., Hey, D., and Evans, L. (1999). Gas chemistry of hydrothermal fluids along the East Pacific Rise, 5°S to 32°S (abstract). *Eos Trans.* 80:F1099. Fall Meet., Suppl.

Mandalakis, M., Gavriilidou, A., Polymenakou, P. N., Christakis, C., Nomikou, P., Medvecký, M., et al. (2019). CO_2 vents at Kolumbo submarine volcano show microbial co-tolerance to high acidity and antibiotics. *Mar. Environ. Res* in press,

Mango, F. D. (2000). The origin of light hydrocarbons. *Geochim. Cosmochim. Acta* 51, 1549–1560. doi: 10.1016/S0016-7037(99)00389-0

Marty, B. (2012). The origins and concentrations of water, carbon, nitrogen and noble gases on Earth. *Earth Planet. Sci. Lett.* 31, 56–66. doi: 10.1016/j.epsl.2011.10.040

Marty, B., and Jambon, A. (1987). C/3He in volatile flux from the solid Earth: implications for carbon dynamics. *Earth Planet. Sci. Lett.* 83, 16–26. doi: 10.1016/0012-821X(87)90047-1

Mazzini, A., Svensen, H., Etiope, E., Onderdonk, N., and Banks, D. (2011). Fluid origin, gas fluxes and plumbing system in the sediment-hosted Salton Sea Geothermal System (California, USA). *J. Volcanol. Geothermal Res.* 205, 67–83. doi: 10.1016/j.jvolgeores.2011.05.008

McCollom, T. M., and Seewald, J. S. (2007). Abiotic synthesis of organic compounds in deep-sea hydrothermal environments. *Chem. Rev*. 107, 382–401. doi: 10.1021/cr0503660

McDermott, J. M., Seewald, J. S., German, C. R., and Sylva, S. P. (2015). Pathways for abiotic organic synthesis at submarine hydrothermal fields. *PNAS* 112, 7668–7672. doi: 10.1073/pnas.1506295112

McKenzie, D. (1972). Active tectonics of the Mediterranean region. *Geophys. J. R. Astron. Soc.* 30, 109–185. doi: 10.1111/j.1365-246X.1972.tb02351.x

Nicholls, I. A. (1971). Petrology of Santorini Volcano. Cyclades, Greece. *J. Petrol.* 12, 67–119. doi: 10.1093/petrology/12.1.67

Nomikou, P., Carey, S., Papanikolaou, D., Croff Bell, K., Sakellariou, D., Alexandri, M., et al. (2012). Submarine volcanoes of the Kolumbo volcanic zone NE of Santorini Caldera Greece. *Glob. Planet. Change* 9, 135–151. doi: 10.1016/j.gloplacha.2012.01.001

Nomikou, P., Hübscher, C., Papanikolaou, D., Farangitakis, P. G., Ruhnau, M., and Lampridou, D. (2018). Expanding extension, subsidence and lateral segmentation within the Santorini - Amorgos basins during Quaternary: implications for the 1956 Amorgos events, central - south Aegean Sea. Greece. *Tectonophysics* 722, 138–153. doi: 10.1016/j.tecto.2017.10.016

Nomikou, P., Hübscher, C., Ruhnau, M., and Bejelou, K. (2016). Tectonophysics Tectono-stratigraphic evolution through successive extensional events of the Anydros Basin, hosting Kolumbo volcanic field at the Aegean. *Tectonophysics* 671, 202–217. doi: 10.1016/j.tecto.2016.01.021

Nomikou, P., Papanikolaou, D., Alexandri, M., Sakellariou, D., and Rousakis, G. (2013). Submarine volcanoes along the Aegean volcanic arc. *Tectonophysics* 59, 123–146. doi: 10.1128/AEM.01835-08

Oppenheimer, C., Fischer, T. P., and Scaillet, B. (2014). "Volcanic degassing: process and impact," in *Treatise on Geochemistry, The Crust*, 2nd Edn, eds H. D. Holland and K. K. Turekian (Amsterdam: Elsevier), 111–179.

Oulas, A., Polymenakou, P. N., Seshadri, R., Tripp, H. J., Mandalakis, M., Paez-Espino, A. D., et al. (2015). Metagenomic investigation of the geologically unique Hellenic Volcanic Arc reveals a distinctive ecosystem with unexpected physiology. *Environ. Microbiol.* 18, 1122–1136. doi: 10.1111/1462-2920.13095

Ozima, M., and Podosek, F. A. (1983). *Noble Gas Geochemistry*. New York, NY: Cambridge University Press.

Paonita, A., Federico, C., Bonfanti, P., Capasso, G., Inguaggiato, S., Italiano, F., et al. (2013). The episodic and abrupt geochemical changes at La Fossa fumaroles (Vulcano Island, Italy) and related constraints on the dynamics, structure, and compositions of the magmatic system. *Geochim. Cosmochim. Acta* 120, 158–178. doi: 10.1016/j.gca.2013.06.015

Parks, M., Biggs, J., England, P., Mather, T., Nomikou, P., Palamartchouk, K., et al. (2012). Evolution of Santorini Volcano dominated by episodic and rapid fluxes of melt from depth. *Nat. Geosci.* 5, 749–754. doi: 10.1038/NGEO1562

Parks, M. M., Caliro, S., Chiodini, G., Pyle, D. M., Mather, T. A., Berlo, K., et al. (2013). Distinguishing contributions to diffuse CO_2 emissions in volcanic areas from magmatic degassing and thermal decarbonation using soil gas 222Rn–δ13C systematics: application to Santorini volcano, Greece. *Earth Planet. Sci. Lett.* 377, 180–190. doi: 10.1016/j.epsl.2013.06.046

Pe-Piper, G., and Piper, D. J. W. (2007). The South Aegean active volcanic arc: relationships between magmatism and tectonics. *Dev. Volcanol.* 7, 113–133. doi: 10.1016/S1871-644X(05)80034-8

Proskurowski, G., Lilley, M. D., Seewald, J. S., Fruh-Green, G. L., Olson, E. J., Lupton, J. E., et al. (2008). Abiogenic hydrocarbon production at Lost City hydrothermal field. *Science* 319, 604–607. doi: 10.1126/science.1151194

Rayleigh, J. W. S. (1896). Theoretical considerations respecting the separation of gases by diffusion and similar processes. *Philos. Mag.* 42:493. doi: 10.1080/14786449608620944

Rizzo, A. L., Barberi, F., Carapezza, M. L., Di Piazza, A., Francalanci, L., Sortino, F., et al. (2015). New mafic magma refilling a quiescent volcano: evidence from He-Ne-Ar isotopes during the 2011–2012 unrest at Santorini, Greece. *Geochem. Geophys. Geosyst.* 16, 798–814. doi: 10.1002/2014GC005653

Rizzo, A. L., Caracausi, A., Chavagnac, V., Nomikou, P., Polymenakou, P. N., Mandalakis, M., et al. (2016). Kolumbo submarine volcano (Greece): an active window into the Aegean subduction system. *Sci. Rep.* 6:28013. doi: 10.1038/srep28013

Sander, R. (2015). Compilation of Henry's law constants (version 4.0) for water as solvent. *Atmos. Chem. Phys.* 15, 4399–4981. doi: 10.5194/acp-15-4399-2015

Sano, Y., and Marty, B. (1995). Origin of carbon in fumarolic gases from island arcs. *Chem. Geol.* 119, 265–274. doi: 10.1016/0009-2541(94)00097-R

Schoell, M. (1980). The hydrogen and carbon isotopic composition of methane from natural gases of various origins. *Geochim. Cosmochim. Acta* 44, 649–661. doi: 10.1016/0016-7037(80)90155-6

Sigurdsson, H., Carey, S., Alexandri, M., Vougioukalakis, G., Croff, K., Roman, C., et al. (2006). Marine investigations of Greece's Santorini Volcanic Field. *EOS Trans. Am. Geophys. Union* 87:337. doi: 10.1029/2006EO340001

Spandler, C., Martin, L. H. J., and Pettke, T. (2012). Carbonate assimilation during magma evolution at Nisyros (Greece), South Aegean Arc: evidence from clinopyroxenite xenoliths. *Lithos* 146, 18–33. doi: 10.1016/j.lithos.2012.04.029

Stucker, V. K., Walker, S. L., de Ronde, C. E. J., Caratori Tontini, F., and Tsuchida, S. (2017). Hydrothermal venting at Hinepuia submarine volcano, Kermadec arc: understanding magmatic-hydrothermal fluid chemistry. *Geochem. Geophys. Geosyst.* 18, 3646–3661. doi: 10.1002/2016GC006713

Stull, D. R., Westrum, E. F., and Sinke, G. G. (1969). *The Chemical Thermodynamics of Organic Compounds*. Hoboken, NJ: Wiley.

Taran, Y., Torokhov, P., Pokrovski, G., and Shabayeva, I. (1992). Isotopic composition of mineral precipitates and free gas associated with hydrothermal vents of Piip submarine volcano, Bering Sea. *Geochem. J.* 26, 291–297. doi: 10.2343/geochemj.26.291

Taran, Y. A., and Giggenbach, W. F. (2003). "Geochemistry of light hydrocarbons in subduction-related volcanic and hydrothermal fluids," in *Volcanic, Geothermal, and ore Forming Fluids: Rulers and Witnesses of Processes within the Earth*, Vol. 10, eds S. F. Simmons and I. J. Graham (Littleton, CO: Economic Geologists Special Publication), 61–74.

Taran, Y. A., Kliger, G. A., Cienfuegos, E., and Shuykin, A. N. (2010a). Carbon and hydrogen isotopic compositions of products of open-system catalytic hydrogenation of CO_2: implications for abiogenic hydrocarbons in Earth's crust. *Geochim. Cosmochim. Acta* 74, 6112–6125. doi: 10.1016/j.gca.2010.08.012

Taran, Y. A., Varley, N. R., Inguaggiato, S., and Cienfuegos, E. (2010b). Geochemistry of H_2- and CH_4-enriched hydrothermal fluids of Socorro Island, Revillagigedo Archipelago, Mexico. Evidence for serpentinization and abiogenic methane. *Geofluids* 10, 542–555. doi: 10.1111/j.1468-8123.2010.00314.x

Tassi, F., Capaccioni, B., Caramanna, G., Cinti, D., Montegrossi, G., Pizzino, L., et al. (2009). Low-pH waters discharging from submarine vents at Panarea Island (Aeolian Islands, southern Italy) after the 2002 gas blast: origin of hydrothermal fluids and implications for volcanic surveillance. *Appl. Geochem.* 24, 246–254. doi: 10.1016/j.apgeochem.2008.11.015

Tassi, F., Capaccioni, B., and Vaselli, O. (2014). Compositional spatial zonation and 2005–2013 temporal evolution of the hydrothermal-magmatic fluids from the submarine fumarolic field at Panarea Island. *J. Volcanol. Geothermal Res*. 277, 41–50. doi: 10.1016/j.jvolgeores.2014.03.010

Tassi, F., Fiebig, J., Vaselli, O., and Nocentini, M. (2012). Origins of methane discharging from volcanic-hydrothermal, geothermal and cold emissions in Italy. *Chem. Geol.* 31, 36–48. doi: 10.1016/j.chemgeo.2012.03.018

Tassi, F., Vaselli, O., Papazachos, C. B., Giannini, L., Chiodini, G., Vougioukalakis, G. E., et al. (2013). Geochemical and isotopic changes in the fumarolic and submerged gas discharges during the 2011–2012 unrest at Santorini caldera (Greece). *Bull. Volcanol* 75, 1–15. doi: 10.1007/s00445-013-0711-8

Tsunogai, U., Ishibashia, J., Wakitaa, H., Gamob, T., Watanabec, K., Kajimurac, T., et al. (1994). Peculiar features of Suiyo Seamount hydrothermal fluids, Izu-Bonin Arc: differences from subaerial volcanism. *Earth Planet. Sci. Lett* 126, 289–301. doi: 10.1016/0012-821X(94)90113-9

Varekamp, J. C., and Buseck, P. R. (1981). Mercury emissions from Mount St. Helens during September 1980. *Nature* 293, 555–556. doi: 10.1038/293555a0

Von Damm, K. L. (1995). "Controls on the chemistry and temporal variability of seafloor hydrothermal fluids," in *Seafloor Hydrothermal Systems: Physical, Chemical, Biological, and Geological Interactions*, Vol. 91, eds S. E. Humphris, R. A. Zierenberg, L. S. Mullineaux, and R. E. Thomson (Washington, DC: AGU), 222–247.

Von Damm, K. L., Oosting, S. E., Kozlowski, R., Buttermore, L. G., Colodner, D. C., Edmonds, H. N., et al. (1995). Evolution of East Pacific Rise hydrothermal vent fluids following a volcanic eruption. *Nature* 375, 47–50. doi: 10.1038/375047a0

Wang, D. T., Reeves, E. P., McDermott, J. M., Seewald, J. S., and One, S. (2018). Clumped isotopologue constraints on the origin of methane at seafloor hot springs. *Geochim. Cosmochim. Acta* 223, 141–158. doi: 10.1016/j.gca.2017.11.030

Welhan, J. A. (1988). Origins of methane in hydrothermal systems. *Chem. Geol.* 71, 183–198. doi: 10.1016/0009-2541(88)90114-3

Wen, H.-Y., Sano, Y., Takahata, N., Tomonaga, Y., Ishida, A., Tanaka, K., et al. (2016). Helium and methane sources and fluxes of shallow submarine hydrothermal plumes near the Tokara Islands, Southern Japan. *Sci. Rep.* 6:34126. doi: 10.1038/srep34126

Whiticar, M. J. (1999). Carbon and hydrogen isotope systematics of bacterial formation and oxidation of methane. *Chem. Geol.* 161, 291–314. doi: 10.1016/S0009-2541(99)00092-3

Xue-Gang, C., Hai-Yan, Z., Xiaohu, L., Chen-Tung, A., Chen, T., Frank, Y., et al. (2016). The chemical and isotopic compositions of gas discharge from shallow-water hydrothermal vents at Kueishantao, offshore northeast Taiwan. *Geochem. J.* 50, 341–355. doi: 10.2343/geochemj.2.0425

Yang, T. F., Lan, T. F., Hsiao-Fen, L., Ching-Chou, F., Pei-Chuan, C., Ching-Hua, L., et al. (2005). Gas compositions and helium isotopic ratios of fluid samples around Kueishantao, NE offshore Taiwan and its tectonic implications. *Geochem. J.* 39, 469–480. doi: 10.2343/geochemj.39.469

Zhang, J., Quay, P. D., and Wilbur, D. O. (1995). Carbon isotope fractionation during gas-water exchange and dissolution of CO_2. *Geochim. Cosmochim. Acta* 59, 107–114. doi: 10.1016/0016-7037(95)91550-D

Conflict of Interest Statement: The authors declare that the research was conducted in the absence of any commercial or financial relationships that could be construed as a potential conflict of interest.